Redox Biology 19 (2018) 339–353

Contents lists available at ScienceDirect

Redox Biology

journal homepage: www.elsevier.com/locate/redox

Sirtuin 3-dependent mitochondrial redox homeostasis protects against AGEs-induced intervertebral disc degeneration

Yu Song[a,1], Shuai Li[a,1], Wen Geng[b,1], Rongjin Luo[a], Wei Liu[c], Ji Tu[a], Kun Wang[a], Liang Kang[a], Huipeng Yin[a], Xinghuo Wu[a], Yong Gao[a], Yukun Zhang[a], Cao Yang[a,*]

[a] Department of Orthopaedics, Union Hospital, Tongji Medical College, Huazhong University of Science and Technology, Wuhan 430022, China
[b] Department of Ophthalmology, Shengjing Hospital, China Medical University, Shenyang 110004, China
[c] Department of Orthopaedics, First Hospital of Wuhan, Wuhan 430022, China

ARTICLE INFO

Keywords:
Mitochondrial redox homeostasis
Intervertebral disc degeneration
Sirtuin 3
Advanced glycation end products

ABSTRACT

Intervertebral disc (IVD) degeneration contributes largely to pathoanatomical and degenerative changes of spinal structure that increase the risk of low back pain. Apoptosis in nucleus pulposus (NP) can aggravate IVD degeneration, and increasing studies have shown that interventions targeting NP cell apoptosis can ameliorate IVD degeneration, exhibiting their potential for use as therapeutic strategies. Recent data have shown that advanced glycation end products (AGEs) accumulate in NP tissues in parallel with the progression of IVD degeneration and form a microenvironment of oxidative stress. This study examined whether AGEs accumulation aggravates NP cell apoptosis and IVD degeneration, and explored the mechanisms underlying these effects. We observed that the viability and proliferation of human NP cells were significantly suppressed by AGEs treatment, mainly due to apoptosis. Furthermore, activation of the mitochondrial apoptosis pathway was detected after AGEs treatment. In addition, the molecular data showed that AGEs could significantly aggravate the generation of mitochondrial reactive oxygen species and prolonged activation of the mitochondrial permeability transition pore, as well as the increased level of Bax protein and decreased level of Bcl-2 protein in mitochondria. These effects could be reduced by antioxidant (2-(2,2,6,6-Tetramethylpiperidin-1-oxyl-4-ylamino)-2-oxoethyl) triphenylphosphonium chloride (MitoTEMPO) and Visomitin (SKQ1). Importantly, we identified that impairment of Sirtuin3 (SIRT3) function and the mitochondrial antioxidant network were vital mechanisms in AGEs-induced oxidative stress and secondary human NP cell apoptosis. Finally, based on findings that nicotinamide mononucleotide (NMN) could restore SIRT3 function and rescue human NP cell apoptosis through adenosine monophosphate-activated protein kinase and peroxisome proliferator-activated receptor-γ coactivator 1α (AMPK-PGC-1α) pathway in vitro, we confirmed its protective effect on AGEs-induced IVD degeneration in vivo. In conclusion, our data demonstrate that SIRT3 protects against AGEs-induced human NP cell apoptosis and IVD degeneration. Targeting SIRT3 to improve mitochondrial redox homeostasis may represent a potential therapeutic strategy for attenuating AGEs-associated IVD degeneration.

1. Introduction

Intervertebral disc (IVD) degeneration and secondary pathological changes in the spinal structure contribute largely to low back pain, which ranks first among the five leading causes of years lived with disability [1]. As the principal intervertebral junction, the

Abbreviations: IVD, intervertebral disc; NP, nucleus pulposus; SIRTs, Sirtuins; AGEs, advanced glycation end products; NMN, nicotinamide mononucleotide; SKQ1, Visomitin; MitoTEMPO, (2-(2,2,6,6-Tetramethylpiperidin-1-oxyl-4-ylamino)-2-oxoethyl) triphenylphosphonium chloride; AMPK, adenosine monophosphate-activated protein kinase; PGC-1α, peroxisome proliferator-activated receptor-γ coactivator 1α; Cyt-c, Cytochrome c; SOD2, superoxide dismutase 2; TRX2, thioredoxin 2; TRXR2, thioredoxin reductase 2; VDAC, voltage-dependent anion channel; GAPDH, glyceraldehyde-3-phosphate dehydrogenase; CCK-8, Cell Counting Kit-8; EdU, 5-Ethynyl-2'-deoxyuridine; TUNEL, TdT-mediated dUTP nick end labeling; MMP, mitochondrial membrane potential; mPTP, mitochondrial permeability transition pore; ROS, reactive oxygen species

* Correspondence to: Department of Orthopaedics, Union Hospital, Tongji Medical College, Huazhong University of Science and Technology, No. 1277 Jiefang Avenue, Wuhan 430022, Hubei, China.
E-mail address: caoyangunion@hust.edu.cn (C. Yang).
[1] These authors contributed equally to the study.

https://doi.org/10.1016/j.redox.2018.09.006
Received 26 April 2018; Received in revised form 3 September 2018; Accepted 5 September 2018
Available online 06 September 2018

fibrocartilaginous property of IVD allows it to buffer the different patterns of mechanical stress, in which the corresponding redistribution of gelatinous NP tissue plays an important role [2]. The resident NP cells are the main executors that control the extracellular matrix metabolism in NP tissue and the collagen II and proteoglycan they produce are the main molecules that maintain the gelatinous property of NP tissue [3,4]. The increased NP cell death partially due to apoptosis may contribute to the metabolic disorders of extracellular matrix, which was seen along with IVD degeneration [4,5]. Furthermore, increasing studies indicated that the interventions targeting NP cell apoptosis could alleviate the metabolic disorders and IVD degeneration [6,7]. Therefore, more investigation on NP cell apoptosis and the target interventions may not only increase the pathogenetic knowledge of IVD degeneration, but also provide potential therapeutic strategy.

Recently, increasing evidence has verified the presence of oxidative stress and increased concentrations of oxidation products in aged and degenerated IVDs [8–10]. Additionally, oxidative stress and subsequent mitochondrial dysfunction participate in the intrinsic pathway of cellular apoptosis, and their roles have been confirmed in NP cell death and IVD degeneration induced by various risk factors [11–13]. Although various interventions targeting oxidative stress and mitochondrial dysfunction have shown beneficial effects on NP cell apoptosis and IVD degeneration [14,15], the detailed mechanisms underlying these disorders are not clear.

Sirtuins (SIRTs) comprise a class of NAD^+-dependent deacetylases with seven members, which share the same conserved NAD^+-binding site and a Sir2 catalytic core domain, and regulate a wide variety of biological functions [16]. Among them, the SIRT3, SIRT4, and SIRT5 members are mainly localized in the mitochondria, with SIRT3 being the best characterized and possessing robust deacetylase activity that is closely related to maintaining mitochondrial redox homeostasis and functional integrity [17]. Impaired SIRT3 function has been found in various diseases associated with oxidative stress and mitochondrial dysfunction, including cardiac hypertrophy, acute kidney injury, and osteoarthritis [18–20]. In addition, nicotinamide mononucleotide (NMN), as a key NAD^+ precursor in mammals, could normalize the NAD^+/NADH ratio and its administration have shown protective effect on oxidative stress-related diseases through manipulating the activity of SIRT members [21–23]. Previously, the studies by our group and others have demonstrated that the accumulation of advanced glycation end products (AGEs) in NP tissues could induce an oxidative microenvironment and mitochondrial dysfunction, which were closely related to IVD degeneration [24–26]. However, the role of SIRT3 in this process and the related mechanism in regulating the survival and proliferation of NP cells have not been examined.

In this study, we reported that in vitro AGEs treatment suppressed the survival and proliferation of human NP cells through induction of oxidative stress and mitochondrial dysfunction, in which the impairment of SIRT3 function and mitochondrial antioxidant network play an important role. The suppression of AMPK/PCG-1α induced by AGEs was involved in this process. Furthermore, NMN supplementation exhibited a protective effect on AGEs-induced NP cell apoptosis and IVD degeneration, partly through the restoration of SIRT3 function and mitochondrial redox homeostasis. Our discoveries provide novel insights into the mechanism of oxidative stress and apoptosis in NP cells, with therapeutic implications for treating IVD degeneration.

2. Materials and methods

2.1. Study design and Ethics statement

Human NP tissues were obtained from patients who underwent intervertebral fusion surgery due to lumbar spinal stenosis, lumbar disc herniation or idiopathic scoliosis. Correspondingly, the patients' medical records were also collected and magnetic resonance images were used to evaluate the IVD degenerative level according to Pfirrmann MRI-grade system [27]. Once isolated, the NP tissue samples were handled according to their intended use. Generally, 14 human NP tissues collected from 6 males and 8 females, aged 16–64 years (mean: 48.6 years) were preserved for immunohistochemical and western blotting analysis. Among them, five tissues evaluated as Grade II were from patients with idiopathic scoliosis; three evaluated as Grade III from patients with lumbar disc herniation; three evaluated as Grade IV and three evaluated as Grade V from patients with lumbar spinal stenosis and lumbar disc herniation. All of them were separated into two parts, immersed in RNAlater Stabilization Solution and frozen in liquid nitrogen for protein and RNA analysis, fixed using buffered formaldehyde fixation (4%, pH 7.4) and embedded in paraffin for histological analysis. Specially, the NP tissues from idiopathic scoliosis patients were generally evaluated as Grade II and also regarded as healthy, another three of which were preserved to isolate NP cells for the further in vitro experiments. Further, we assessed the IVD degenerative events in vivo using rat tail disc degeneration model.

All experimental protocols involving human IVD, including medical records, NP tissue collection and analysis, NP cell isolation and interventions, were approved by the Ethics Committee of Tongji Medical College, Huazhong University of Science and Technology (NO. S214). The animal experiments were performed following a protocol approved by the Animal Experimentation Committee of Huazhong University of Science and Technology.

2.2. Isolation and culture of human NP cells

Three human NP tissues used for NP cell isolation were described as above. Hank's balanced salt solution was used for NP tissue transportation, and subsequent cell isolation was performed as described previously [28], by plating and expanding the cells at 37 °C and 5% CO_2 in Dulbecco's modified Eagle's medium with the F12 nutrient mixture containing 15% fetal bovine serum (Gibco, Waltham, MA, USA) and 1% penicillin/streptomycin (Invitrogen). Cells from the second passage were identified using fluorescently labeled antibody for NP cell markers [29] (CD24, ab31622; KRT18, ab215839; Abcam, Cambridge, UK) and used in further experiments. In in vitro experiments, NP cells were exposed to an equal volume of phosphate-buffered saline (PBS) or AGEs (100 μg/ml or 200 μg/ml buffered using PBS; Merck Millipore, Darmstadt, Germany) for 0, 12, 24, or 36 h. Cells were either pre-treated with MitoTEMPO (5 μM; Sigma, Shanghai, China) or SKQ1 (20 nM; MedChemExpress, New Jersey, USA) for 2 h and then treated with PBS or AGEs, or directly co-cultured with PBS or AGEs in combination with NMN (100 μM), A-769662 (50 μM), Compound C (50 uM; MedChemExpress) or RAGE antibody (10 μg/ml; R&D Systems, Minneapolis, USA). To knock down SIRT3 expression, cells were transfected for 48 h with 100 nM SIRT3 small-interfering RNA (siRNA) or scrambled siRNA (GenePharma, Shanghai, China) using Lipofectamine 2000 (Invitrogen) and immediately stimulated with PBS or AGEs. In addition, lentiviral plasmid containing the SIRT3 expression (Lenti-SIRT3) vector and flanking sequence control (Lenti-vector) were purchased from GeneChem (Shanghai, China) and transduced into human NP cells following the manufacturer's instructions. Transfection efficacies were detected by western blotting and the cells were further cultured for 3 days, and passaged for subsequent experiments.

2.3. Assessment of human NP cell viability and proliferation

Cell viability assessment was performed as described previously [30], using a Cell Counting Kit-8 (CCK-8; CK04, Dojindo, Japan). After treatment with PBS or AGEs, CCK-8 solution (10 μl) was added to each well, and the cells were further cultured for 4 h at 37 °C. Absorbance in the wells was measured at 450 nm using a spectrophotometer (BioTek, Winooski, VT, USA).

NP cell proliferation was also detected by 5-ethynyl-2′-deoxyuridine (EdU) incorporation (C10310-3; Ribobio, Guangzhou, China). The

assessment was performed as the procedure recommended by the manufacturer and fluorescent images were finally obtained by a fluorescence microscope (Olympus IX71, Tokyo, Japan).

2.4. Analysis of human NP cell apoptosis

An Annexin V-APC/7-AAD Apoptosis Detection Kit (40309ES60; Yeasen biotech) was used in the analysis of apoptosis as previously described [28]. After labeled, all samples were applied to FACSCalibur flow cytometer (BD Biosciences, San Jose, CA, USA) and analyzed. Moreover, apoptotic cells were also identified by 5-ethynyl-2′-deoxyuridine (EdU)-incorporation, terminal deoxynucleotidyl transferase dUTP nick-end labeling (TUNEL) staining method using the In Situ Cell Death Detection Kit (12156792910; Roche Applied Science, Indianapolis, IN, USA), according to the manufacturer's instructions. Fluorescent images were finally obtained by a fluorescence microscope (Olympus IX71).

2.5. Assessment of reactive oxygen species (ROS), mitochondrial membrane potential (MMP) and mitochondrial permeability transition pore (mPTP) activity in human NP cells

The intracellular total and mitochondrial ROS level were measured respectively by 2',7'-dichlorofluorescin diacetate (DCFH-DA, S0033; Beyotime, Beijing, China) and MitoSOX (40778ES50; Yeasen biotech, Shanghai, China) staining. Both of them can be rapidly oxidized to highly fluorescent compounds. The samples were stained according to the manufacturers' instructions and detected by FACSCalibur flow cytometer (BD Biosciences). Further, the mitochondrial ROS was evaluated by the colocalization of MitoSOX and Mitotracker (C1048, Beyotime) intensity detected using Laser Scanning Microscope (ZEISS LSM780, Germany).

MMP was detected using JC-1 (C2006; Beyotime) assay kits as described previously [30] and analyzed by FACSCalibur flow cytometer (BD Biosciences). The decrease ratio of red (JC-1 aggregates) to green (JC-1 monomers) indicated the MMP loss. The mPTP Assay Kit (GMS10095.1; Genmed, Shanghai, China) was used to detect mPTP activity, wherein fluorescence quenching by cobalt ions increased when the mPTP activity increased. NP cell staining and fixation were performed according to the manufacturer's instructions. Next, the slides were observed and imaged using a fluorescence microscope (Olympus IX71).

2.6. Western blotting for human NP cells

Total proteins, cytoplasmic proteins, and mitochondrial proteins were extracted using corresponding kits (Beyotime). Proteins (40 μg) from each sample were electrophoresed on 4–20% precast polyacrylamide gels (Bio-Rad) and transferred to nitrocellulose membranes (Bio-Rad, Hercules, CA, USA). The primary antibodies were diluted from 1: 500–1: 1000. Primary antibodies against the following proteins were used: cleaved Caspase-3 (#9664), GAPDH (#5174) and SIRT3 (#2627S) (Cell Signaling Technology; Danvers, MA, USA); cytochrome C (ab110325), Bcl-2 (ab32124), and Bax (ab32503) (Abcam, Cambridge, UK); SOD2 (sc-133134), mitochondrial thioredoxin 2 (TRX2, sc-137028), mitochondrial thioredoxin reductase 2 (TRXR2, sc-166259), catalase (sc-271358), and VDAC1 (sc-32063) (Santa Cruz Biotechnology; Dallas, TX, USA).

2.7. SIRT3 deacetylase-activity assay in human NP cells

The deacetylase activity of SIRT3 was determined with a SIRT3 Fluorescent Activity Assay/Drug Discovery Kit (BML-AK557-0001; Enzo Life Sciences, Plymouth Meeting, PA, USA), following the manufacturer's protocol. Briefly, the mitochondrial extract (5 μg) was incubated with the FLUOR DE LYS®-SIRT2 buffer at 37 °C for 60 min, followed by incubation with FLUOR DE LYS® Developer II buffer at 37 °C for 40 min. The fluorescence intensity was measured using a microtiter plate fluorimeter, with excitation at 360 nm and emission at 460 nm. The "blank" value of assay buffer was subtracted from all other values.

2.8. Surgical procedure in animal models

Sprague–Dawley rats (three months old) were obtained from the Laboratory Animal Center of Huazhong University of Science and Technology (Wuhan, China). The surgical procedure was performed as described previously [14]. After rats were anesthetized with 2% (w/v) pentobarbital (40 mg/kg), the disc levels in rat tail (Co6/7, 7/8, and 8/9) were located by palpation on the coccygeal vertebrae and confirmed by trial radiography. Needles (29-G) were used to puncture the annulus fibrosus layer though the tail skin, in parallel to the end plates. To ensure that the needle did not penetrate too deeply, the length of the needle was pre-determined according to the dimensions of annulus fibrosus and the NP, which were measured in a preliminary experiment and found to be approximately 4 mm. To evaluate the effect of AGEs on NP cell survival and IVD degeneration and the therapeutic potential of NMN treatment in vivo, we prepared three solutions for intradisc injection, including PBS, AGEs (200 μg/ml), and a mixture of AGEs (200 μg/ml) and NMN (100 μM). Each segment was injected with 2 μl of the solution of interest, and each needle were kept in the disc for 10 s. All animals were allowed free, unrestricted weight bearing and activity. The injections were conducted each week for one month.

2.9. Magnetic resonance imaging and degenerative grade analysis in animal models

Magnetic resonance imaging (MRI) of the target IVD was performed one-month after surgery. All rats were anesthetized with 2% (w/v) pentobarbital (40 mg/kg) and placed on examination couch with their tails straightened. Then, the imaging was performed at T2-weighted signal using BioSpec MRI (Bruker, 7.0 T/20 cm). T2-weighted parameters were set as followed: a fast-spin echo sequence with a time-to-repetition of 2000 ms and a time-to-echo of 36 ms; a 256 (h) × 256 (v) matrix; a field of view 6.00/3.00 cm; a flip angle 180°. The scanning scope consisted of 6 IVDs, including 3 target segments. The IVD degenerative grades were analyzed with MR images according to Pfirrmann MRI-grade system [27]. Briefly, Grade I: homogeneous disc with bright hyperintense white signal intensity and a normal disc height; Grade II: inhomogeneous disc with or without horizontal bands and a hyperintense white signal; Grade III: inhomogeneous disc with intermediate gray signal intensity and a slightly decreased disc height; Grade IV: inhomogeneous disc with hypointense gray or black signal intensity and a moderately decreased disc height; Grade V: inhomogeneous disc with a hypointense black signal intensity and a collapsed disc space. Then, the rats were euthanized and the discs were harvested for histological and immunohistochemical analysis.

2.10. Histological, immunohistological and western blotting analysis in human NP tissues and animal models

For western blotting analysis, the frozen tissues were homogenized and used for extracting total protein. The next procedure was performed as above. For immunohistochemical analysis, the tissue paraffin blocks were sectioned at 4 μm and handled as described previously [28]. Sections were probed at 4 °C overnight with primary antibody (diluted 1: 200) against AGEs (ab23722, Abcam), washed thoroughly, and labeled for 40 min at 37 °C with an appropriate secondary antibody (diluted 1: 200; Vector, Burlingame, CA, USA). The section of brachial artery tissue from a 60-year-old patient due to trauma and amputation was used as positive control handled as above. The negative controls included parallel sections treated with PBS solution instead of primary

antibody. Images were captured and further analyzed using Image-Pro Plus software, version 6.0.

The rat discs were washed in PBS, fixed with buffered formaldehyde (4%, pH 7.4) for 12 h, decalcified in 10% formic acid solution, dehydrated through a graded series of ethanol, and embedded in paraffin. For The specimens were sectioned at 4 μm. For histological analysis, the sections were deparaffinized, rehydrated, and stained with hematoxylin and eosin (HE) and safranin-O (SO). For immunofluorescence staining, the sections were handled as above with primary antibody against SIRT3 (10099-1-AP, 1:50, Proteintech, China) and cleaved-caspase-3 (1:200). After overnight, the sections were washed thoroughly using PBST and labeled with an appropriate secondary antibody. For TUNEL staining, the sections were handled using TUNEL Apoptosis Assay Kit (C1088, Beyotime). Finally, nuclei were co-stained for 5 min with 0.1 g/ml 40,6-diamidino-2-phenylindole, and samples were washed and imaged with a fluorescence microscope (Olympus IX71).

2.11. Statistical analysis

Data were analyzed using SPSS software, version 17.0 (IBM, Chicago, IL, USA) and are reported as the mean ± SD of at least three independent experiments. Non-parametric linear regression was used to assess the correlation among SIRT3 levels, the Pfirrmann grades and the AGEs levels in the clinical samples. Student's *t*-test, one-way or two-way analysis of variance was used to compare data from the in vitro experimental groups. Values of $P < 0.05$ were considered to represent statistically significant differences.

3. Results

3.1. AGEs treatment attenuated cell viability and proliferation, and promoted apoptosis in human NP cells

AGEs can enhance protein cross-links to change the mechanical properties of the extracellular matrix and to act as a ligand to induce pathophysiological reactions (such as inflammatory responses, senescence, and autophagy), which are partially observed in IVD tissues [24,31]. To further investigate the effect of AGEs on the viability of NP cells, we firstly isolated human NP cells and identified them using flow cytometry. The results showed positive CD24 (94.2%) and KRT18 (96.7%) expression (Fig. S1). Human NP cells were then cultured with AGEs (100 or 200 μg/ml) for 12, 24, or 36 h, because this dosage has previously been proven to be sufficient for inducing biological events in chondrocytes, dermal fibroblasts, and lens epithelial cells [32–34]. The CCK-8 assay revealed that viability of NP cells significantly decreased after AGEs treatment in time- and dose-dependent manners (Fig. 1A). In addition, another fast and sensitive method for DNA synthesis detection (EdU-incorporation) was used to observe NP cell proliferation [35]. As shown in Fig. 1B, the activity of DNA replication was significantly attenuated in AGEs-treated groups, indicating the inhibitory effect of AGEs on human NP cell proliferation.

Excessive apoptosis was reported to play an important role in the loss of cell viability and IVD degeneration [5]. Thus, the role of apoptosis in the observed growth inhibition was determined. The results of annexin V-APC and 7-aminoactinomycin D (7-AAD) staining confirmed that AGEs treatment significantly increased apoptosis in human NP cells (Fig. 1C). Additionally, the increased formation of DNA strand breaks (detected by TUNEL staining) also indicated the increased occurrence of apoptosis in AGEs-treated human NP cells (Fig. 1D). Western blotting demonstrated that the level of the apoptotic marker protein, cleaved caspase-3, increased in human NP cells after AGEs treatment (Fig. 1E).

3.2. The mitochondrial pathway was involved in AGEs-induced human NP cell apoptosis

The mitochondrial pathway intrinsically regulates the cell apoptotic events via mitochondrial membrane permeabilization and subsequent release of proapoptotic proteins [36]. Firstly, we examined inner mitochondrial membrane permeability, which could be increased by prolonged mPTP opening. The fluorescence microscopy confirmed that less calcein was retained in mitochondria from AGEs-treated human NP cells compared to that from PBS-treated human NP cells (Fig. 2A), indicating the prolonged mPTP opening. Further, the electrochemical gradient across the inner mitochondrial membrane forms the basis of mitochondrial membrane potential (MMP), which would be reduced by prolonged mPTP opening and inner mitochondrial membrane permeabilization. JC-1 staining and flow cytometric analysis showed that AGEs treatment enhanced the MMP loss in human NP cells, indicated by the decreased ratio of red to green (Fig. 2B), indicating the loss of MMP. Secondly, we examined the ratio of Bcl-2 to Bax protein in mitochondria, of which interaction highly regulated the outer mitochondrial membrane permeabilization. The western blotting results showed that the ratio of Bcl-2 to Bax protein in mitochondria was significantly reduced by AGEs treatment (Fig. 2C). Finally, we examined the cellular localization of proapoptotic protein (cytochrome c, Cyt-c), the release of which (from the mitochondria to the cytoplasm) is critical for the apoptotic event of caspase activation. Western blotting analysis demonstrated that the ratio of mitochondrial to cytoplasmic Cyt-c was significantly reduced by AGEs treatment (Fig. 2D). These data revealed that AGEs affected mitochondrial apoptotic pathway, which was involved in the induction of human NP cell apoptosis in vitro.

3.3. Mitochondrial antioxidants pre-treatment alleviated the level of oxidative stress induced by AGEs treatment and reduced apoptosis in human NP cells

It was previously shown that ROS generation played a vital role in regulating the mitochondrial localization of the pro-apoptotic Bax protein and in prolonging mPTP activation [37,38]. Here, the ROS level was probed using a DCFH-DA Assay Kit and detected by flow cytometry. We observed time-dependent increases in intercellular ROS levels after AGEs treatment, as seen by an increased fluorescence intensity (Fig. 3A). After 36 h of culture, NP cells treated with AGEs showed significantly increased ROS levels compared to those in control cells treated with PBS (Fig. 3A). To further define the source of ROS, we specifically scavenged mitochondrial ROS with the antioxidants Mito-TEMPO or SKQ1. As shown, increased ROS levels induced by AGEs were ameliorated by MitoTEMPO or SKQ1 pre-treatment (Fig. 3B), indicating that mitochondrial ROS contributed partially to oxidative stress in human NP cells treated with AGEs.

To investigate whether mitochondrial ROS participated in AGEs-induced mitochondrial dysfunction and human NP cell apoptosis, we pre-treated human NP cells with MitoTEMPO or SKQ1 for 2 h and then treated them with AGEs for 36 h. The fluorescence microscopy and flow cytometry results showed that MitoTEMPO or SKQ1 pretreatment could alleviate the prolonged mPTP activation and MMP loss induced by AGEs (Fig. 3C and D), as well as the reduced Bcl-2: BAX ratio (Fig. 3E). In addition, attenuated translocation of mitochondrial Cyt-c was detected by western blotting analysis (Fig. 3F). Finally, both annexin V-APC/7-AAD and TUNEL staining confirmed that MitoTEMPO or SKQ1 pre-treatment alleviated AGEs-induced apoptosis in human NP cells (Fig. 4A and B). Collectively, these findings indicated that mitochondrial redox disorder and oxidative stress were involved in AGEs-induced mitochondrial dysfunction and human NP cell apoptosis.

3.4. The SIRT3 protein level negatively correlated with AGEs accumulation and the grade of IVD degeneration

Stable SIRT3 function is important for maintaining mitochondrial redox homeostasis and function, and a deficiency or dysfunction in these processes have been seen in various oxidative stress-related diseases [18,39]. To investigate the role of SIRT3 in IVD degeneration, we

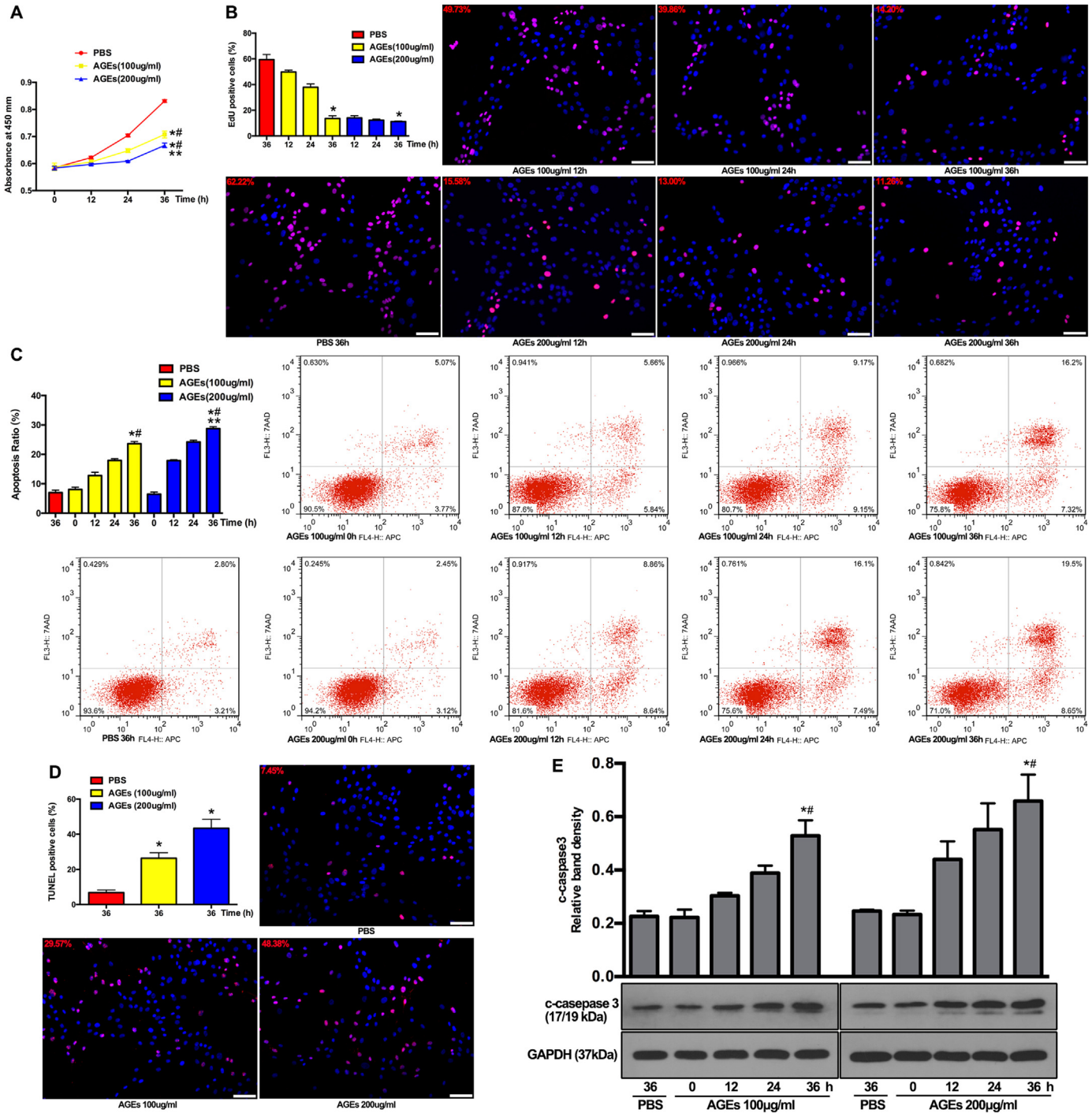

Fig. 1. AGEs treatment inhibited cell viability and proliferation and promoted cell apoptosis. The human NP cells were treated with AGEs (100–200 μg/ml) or PBS for 0–36 h. (A) Cell viability was examined by the absorbance of CCK-8. *p < 0.05 versus PBS (36 h). #p < 0.05 versus 0 h. **p < 0.05 versus AGEs (100 μg/ml at 36 h). (B) Cell proliferation was detected by EdU staining under fluorescence microscope and the positive cells were quantitated. *p < 0.05 versus PBS (36 h). (C, D) Cell apoptosis was detected by Annexin V-APC/7-AAD and TUNEL staining and analyzed using flow cytometry and fluorescence microscope, respectively. (C) The quantitative analysis of apoptosis ratio and representative scatter plots of Annexin V-APC/7-AAD staining. The proportion of live cells (third quadrant), apoptotic cells (first and fourth quadrant) and necrotic cells (second quadrant) was measured for analysis. *p < 0.05 versus PBS (36 h). #p < 0.05 versus 0 h. **p < 0.05 versus AGEs (100 μg/ml at 36 h). (D) The quantitative analysis of TUNEL positive cells and representative fluorescent images with TUNEL staining. *p < 0.05 versus PBS (36 h). (E) Representative Western blotting assay and quantitation of the level of cleaved caspase 3. *p < 0.05 versus PBS (36 h). #p < 0.05 versus 0 h. Scale bar: B, 60 μm; D, 60 μm.

first assessed the SIRT3 levels in human NP tissue specimens with different grades of degeneration (Fig. 5A), according to Pfirrmann MRI-grade system [27]. Non-parametric linear-regression analysis between SIRT3 protein levels and IVD degenerative grades was secondarily performed, and a significant negative correlation was seen (Fig. 5C). As shown above, AGEs contributed largely to a microenvironment of oxidative stress and apoptosis in human NP cells. Previously, it was reported that AGEs showed an increased level in degenerative IVD [40]. In this study, we further analyzed the relationship between AGEs levels and IVD-degeneration grades. As expected, a significant positive

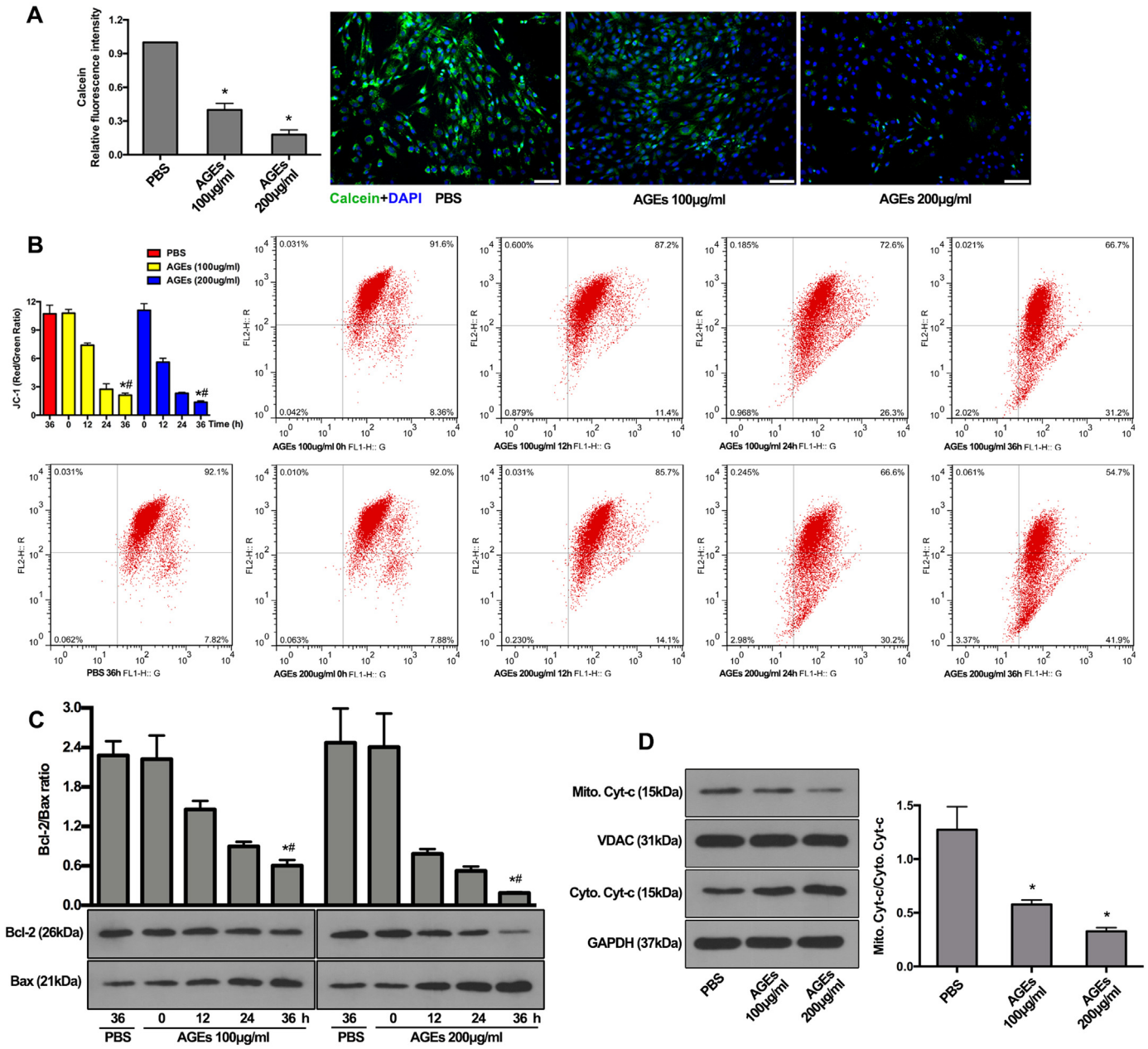

Fig. 2. AGEs treatment induced mitochondrial dysfunction and cytochrome c release via prolonged mPTP activation and Bax translocation at mitochondria. The human NP cells were treated as described in Fig. 1. (A) Representative fluorescent images with calcein staining and quantitative analysis of fluorescence intensity using Image-Pro Plus 6.0 for mPTP. Green fluorescence indicated calcein signals. Cell nuclei are stained by DAPI. *p < 0.05 versus PBS (36 h). (B) The quantitative analysis of the shift of red fluorescence (x axis) to green fluorescence (y axis) for MMP and representative scatter plots of flow cytometry by JC-1 staining. *p < 0.05 versus PBS (36 h). #p < 0.05 versus 0 h. (C) Representative western blotting assay and quantitation of the ratio of Bcl-2/Bax protein in mitochondrial extracts. *p < 0.05 versus PBS (36 h). #p < 0.05 versus 0 h. (D) Representative western blotting assay and quantitation of the level of cytochrome c (Cyt-c) in mitochondrial and cytoplasmic extracts. *p < 0.05 versus PBS. Scale bar: A, 60 μm.

correlation was seen (Fig. 5B and D), with the positive and negative controls in Fig. S2. Moreover, a significant correlation was observed between SIRT3 and AGEs levels (Fig. 5E). These results demonstrated that AGEs-associated IVD degeneration may involve the impairment of SIRT3 function.

3.5. SIRT3 protected human NP cells against oxidative stress and apoptosis induced by AGEs

To determine whether AGEs deposition could affect SIRT3 function during IVD degeneration, we treated human NP cells with AGEs or PBS for 36 h in vitro and examined SIRT3 protein levels and deacetylase activities. Western blotting results showed that AGEs induced dose-dependent decreases in SIRT3 protein levels (Fig. 6A). Similarly, suppression of SIRT3 deacetylase activity was detected in human NP cells following AGEs treatment (Fig. 6B). We further examined the mitochondrial antioxidant network in AGEs-treated human NP cells because of its importance in maintaining the physiological levels of ROS. Moreover, SIRT3 was critical for maintaining the mitochondrial antioxidant network [18,39]. As shown, the members of the mitochondrial antioxidant network, including SOD2, catalase, TRX2, and TRXR2, were significantly suppressed by AGEs treatment in a dose-dependent manner (Fig. 6C). To further confirm the role of SIRT3 in regulating mitochondrial redox homeostasis and apoptosis, we used specific siRNA

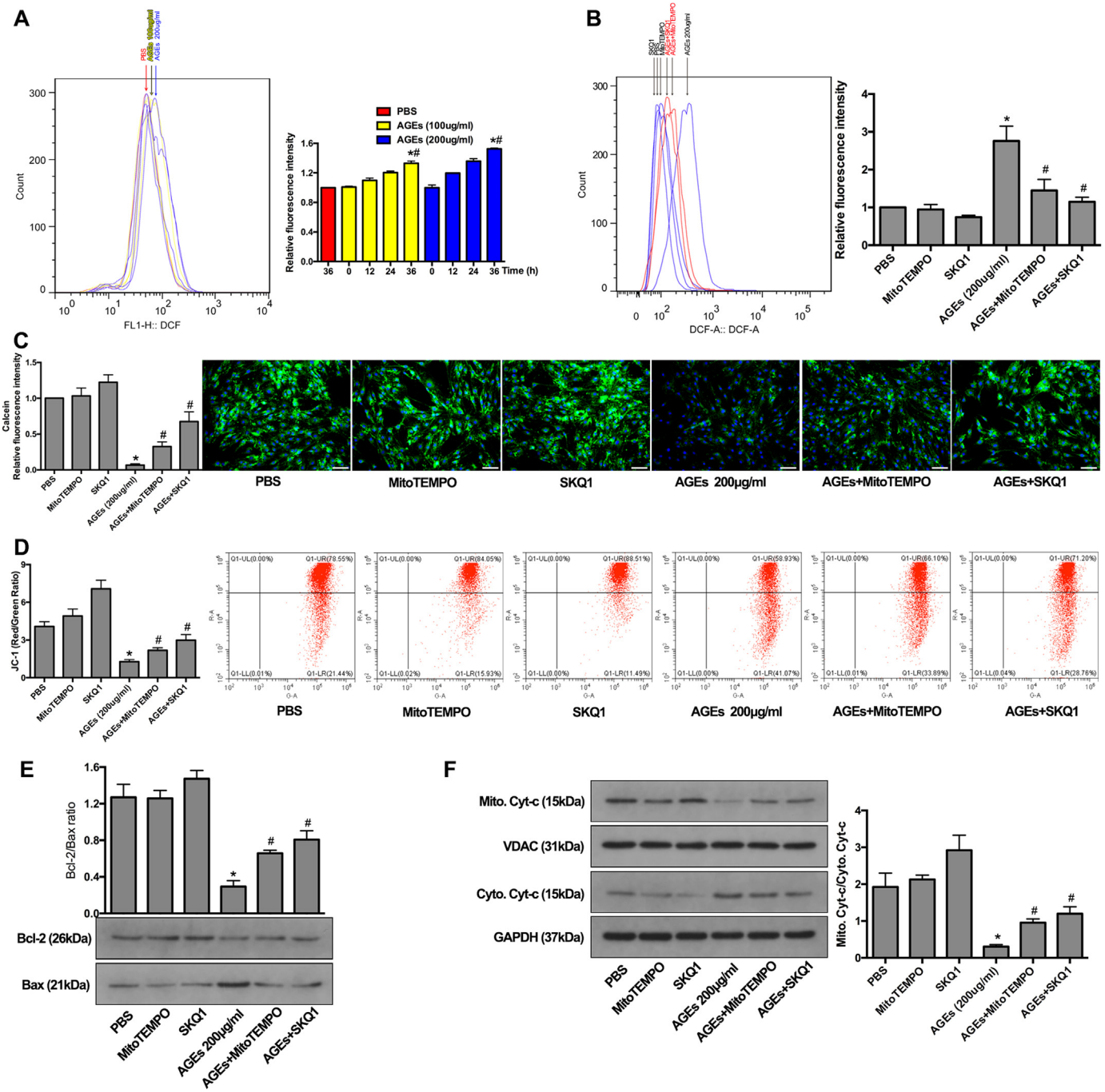

Fig. 3. The alleviation of oxidative stress by MitoTEMPO and SKQ1 inhibited the mitochondrial apoptotic pathway. (A) Human NP cells were treated with AGEs (100–200 μg/ml) or PBS for 0–36 h. Cellular ROS was stained by DCFH-DA and the representative peak charts of flow cytometry and quantitative analysis were shown. *p < 0.05 versus PBS (36 h). #p < 0.05 versus 0 h. (B) MitoTEMPO (5 μM) or SKQ1 (20 nM) pre-treated human NP cells for 2 h and then acted with AGEs (200 μg/ml) for another 36 h. The flow cytometry and quantitative analysis were performed. *p < 0.05 versus PBS. #p < 0.05 versus AGEs (200 μg/ml). (C–D) MitoTEMPO or SKQ1 pre-treatment significantly decreased the mPTP activation (C) and suppressed the MMP loss (D) in AGEs-induced human NP cells, as observed by calcein and JC-1 staining, respectively. *p < 0.05 versus PBS. #p < 0.05 versus AGEs (200 μg/ml). (E) Representative western blotting assay and quantitation of the ratio of Bcl-2/Bax protein in mitochondrial extracts. *p < 0.05 versus PBS. #p < 0.05 versus AGEs (200 μg/ml). (F) Representative western blotting assay and quantitation of the level of Cyt-c in mitochondrial and cytoplasmic extracts from human NP cells with MitoTEMPO or SKQ1 pre-treatment as above. *p < 0.05 versus PBS. #p < 0.05 versus AGEs (200 μg/ml). Scale bar: C, 60 μm.

(siSIRT3) to knock down SIRT3 expression or SIRT3 lentiviral plasmid (Lenti-SIRT3) to overexpression SIRT3 in normal and AGEs-treated human NP cells. Western blotting results confirmed the knockdown efficiency (Fig. 6D), and the corresponding decrease of SIRT3 deacetylase activity was also detected (Fig. 6E). SIRT3 knockdown not only partially mimicked the effect of AGEs on mitochondrial antioxidant network in human NP cells under normal conditions, but also aggravated this effect in AGEs-treated human NP cells (Fig. 6H). In addition, Lenti-SIRT3 infection significantly alleviated the suppressive effect of AGEs on SIRT3 protein levels and deacetylase activities in human NP cells (Fig. 6F and G), as well as on mitochondrial antioxidant network (Fig. 6I). These results showed the critical role of SIRT3 in

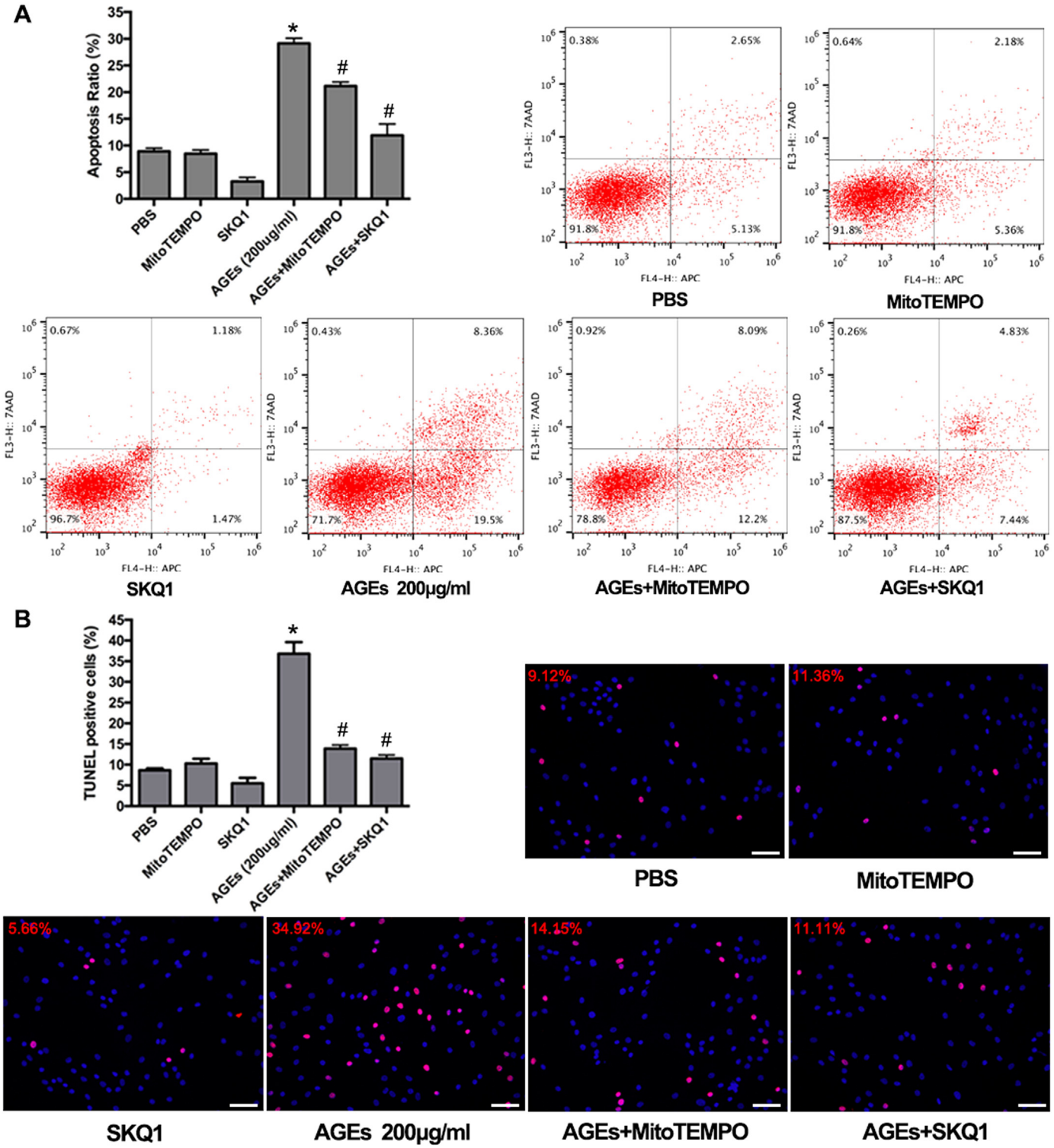

Fig. 4. MitoTEMPO or SKQ1 pre-treatment rescued human NP cell apoptosis induced by AGEs. Respectively, the flow cytometry and fluorescence microscope analysis with Annexin V-APC/7-AAD (A) and TUNEL staining (B) indicated the attenuated apoptosis ratio by MitoTEMPO or SKQ1 pre-treatment. *p < 0.05 versus PBS. #p < 0.05 versus AGEs (200 μg/ml). Scale bar: B, 60 μm.

maintaining mitochondrial antioxidant network and indicated its potential involvement in AGEs-induced oxidative stress and apoptosis in human NP cells.

Thus, we examined the mitochondrial ROS levels by MitoSOX (red) and MitoTracker (green) double-staining. The fluorescence results showed that more co-staining of MitoSOX and MitoTracker was observed in AGEs-treated or siSIRT3-transfected human NP cells and less co-staining was observed in Lenti-SIRT3-infected human NP cells (Fig. 6J and Fig. S3A). Furthermore, the flow cytometry analysis demonstrated that SIRT3 knockdown by siSIRT3 could increase mitochondrial ROS levels and cell apoptosis in normal or AGEs-treated NP cells (Fig. S3B and Fig. 6K), while SIRT3 overexpression by Lenti-SIRT3

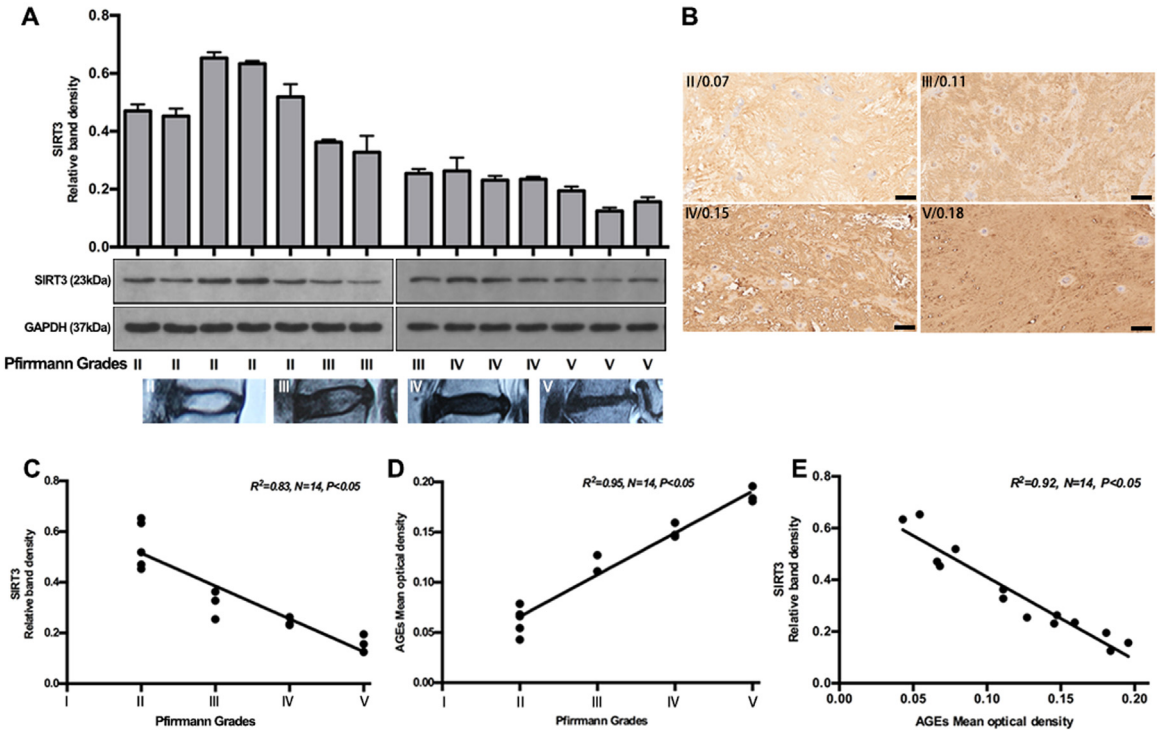

Fig. 5. Decreased SIRT3 protein level negatively correlated with AGEs accumulation and IVD degeneration. Fourteen NP tissue specimens with different degenerative grades were used to analyze SIRT3 and AGEs level by Western blotting and immunohistochemical analysis, respectively. (A) Representative Western blotting assay and quantitation of the levels of SIRT3 (Down: representative MR images with different degenerative grades). (B) Representative immunohistochemical images labeled by AGEs antibody and quantitation by mean optical density using Image-Pro Plus 6.0. (C–E) Correlation analysis among SIRT3, AGEs and Pfirrmann grade was performed successively. Scale bar: B, 100 μm.

ameliorated AGEs-induced mitochondrial oxidative stress and cell apoptosis (Fig. S3C and Fig. 6L). These results indicated that the suppressed SIRT3 function played an important role in AGEs-induced mitochondrial oxidative stress and human NP cell apoptosis and the restoration of SIRT3 function could alleviate these processes.

3.6. Administration of NMN restored SIRT3 function and reduced human NP cell apoptosis through AMPK/PGC-1α pathway

Based on the protective results through SIRT3 gene manipulation, we further investigated the therapeutic potential of pharmacological administration. Previous studies have reported that AMPK/PGC-1α pathway could limit oxidative stress in osteoarthritis progression [41] and PGC-1α was an important transcriptional coactivator for SIRT3 expression [19]. Here, we investigated their interaction in AGEs-induced human NP cell apoptosis. Firstly, the western blotting results showed that AGEs significantly suppressed the AMPK/PGC-1α pathway by decreasing the phosphorylation levels of AMPK and PGC-1α, as well as SIRT3 protein level (Fig. 7A) and AMPK activator A-769662 could ameliorate this suppressive effect (Fig. 7B). In addition, the receptor RAGE was attributed to most cellular events by AGEs. However, RAGE neutralizing antibody did not hamper the downregulation of p-AMPK, p-PGC-1α and SIRT3 induced by AGEs (Fig. 7B). Furthermore, NMN has been reported to act as a precursor of NAD^+ and restore SIRT3 function [21,42]. Importantly, NMN administration has undergone clinical trials for some diseases. Thus, we investigated its role in AGEs-treated human NP cells and examined the mechanisms, combining with AMPK inhibitor (Compound C). As shown, NMN administration could rescue the AGEs-induced suppression on p-AMPK, p-PGC-1α and SIRT3 levels, while Compound C inhibited this protective effect (Fig. 7B). Similarly, both NMN administration and AMPK/PGC-1α pathway activator by A-769662 upregulated the levels of mitochondrial antioxidant members in AGEs-treated human NP cells (Fig. 7C).

To more specifically confirm the essential role of SIRT3 in NMN- and A-769662-induced protective effect, we underwent SIRT3 knockdown before NMN and A-769662 administration. As shown in Fig. 7D, SIRT3 knockdown could significantly inhibit the upregulation of SOD2, catalase, TRX2 and TRXR2 by NMN and A-769662. Finally, the fluorescence microscope and flow cytometry results indicated that NMN and A-769662 administration alleviated AGEs-induced mitochondrial ROS levels and cell apoptosis, which were blocked by SIRT3 knockdown (Fig. 7E and F, Fig. S4). These results demonstrated that the inhibition of AMPK/PGC-1α pathway was involved in AGEs-induced SIRT3 downregulation and NMN supplement could restore SIRT3 function and reduce human NP cell apoptosis through AMPK/PGC-1α pathway.

3.7. Administration of NMN ameliorated IVD degeneration in rat models in vivo

To further investigate the therapeutic efficacy of NMN against AGEs-induced IVD degeneration, we constructed an animal model of IVD degeneration using Sprague-Dawley rats. The degenerative grade was identified by magnetic resonance imaging (MRI, 7.0T) examination and determining Pfirrmann MRI-grade scores. After one month, MRI examination confirmed that the intensities of IVD from AGEs-injected groups were inhomogeneous and lower at T2-weighted signal than that observed in the PBS-injected groups (Fig. 8A), similar as the previous observation [43]. Moreover, the normal disc height and the boundary of nucleus pulposus and annulus fibrosus also disappeared in IVD from AGEs-injected groups. Similarly, the increased degenerative grades evaluated by Pfirrmann MRI-grade system were also seen in AGEs-injected groups (Fig. 8E). In addition, the IVD specimens from the above animal models were subjected to histopathological analysis and scores. As seen in Fig. 8B and C, the oval-shaped NP occupied a large volume of the disc height (> 50%) in the midsagittal cross-section, as detected by HE staining, and a high glycosaminoglycan content was confirmed in

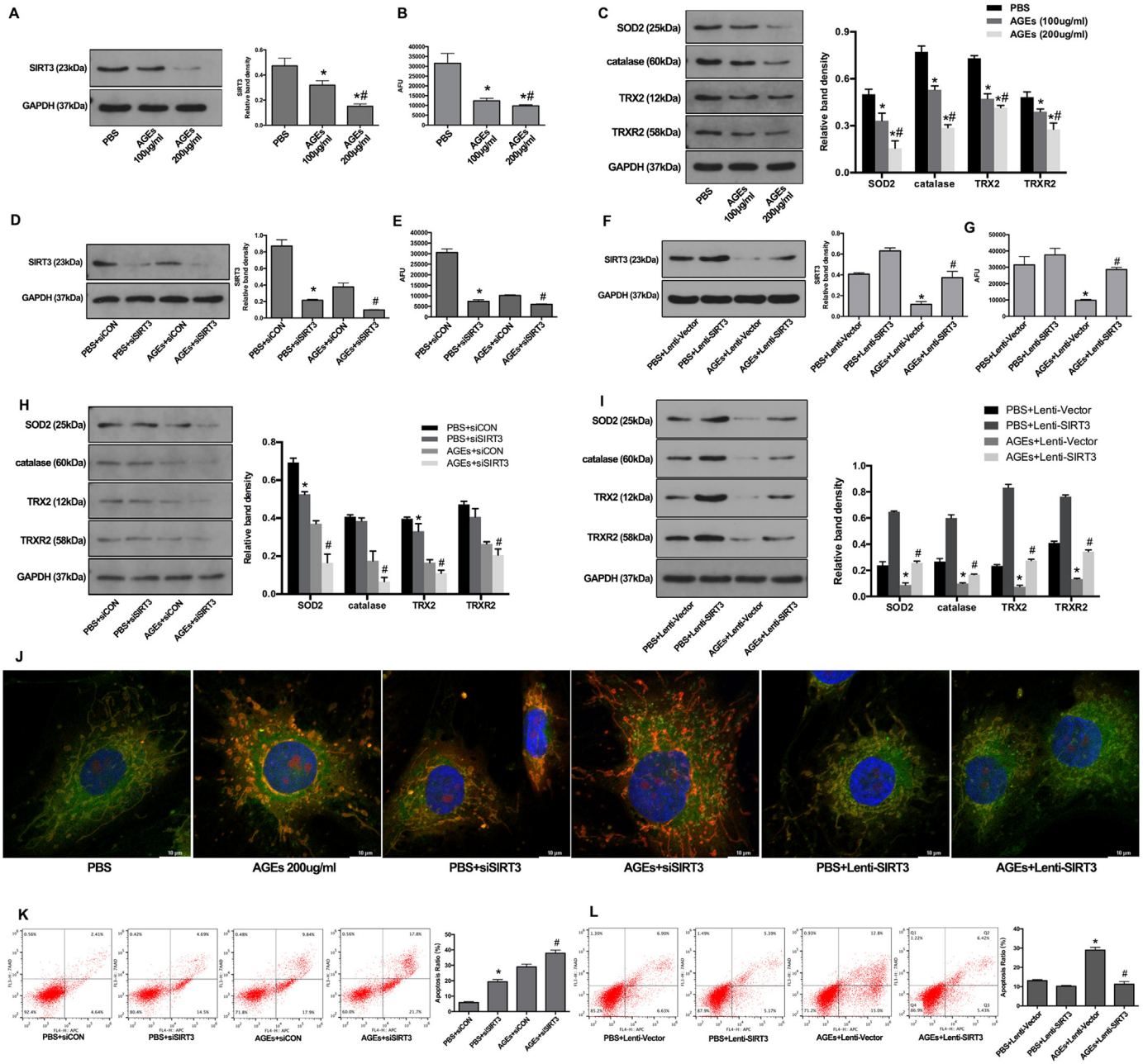

Fig. 6. Impairment of SIRT3 function was involved in AGEs-induced oxidative stress and apoptosis in human NP cells and SIRT3 overexpression could alleviate these processes. (A, B) Human NP cells were treated with AGEs (100–200 μg/ml) or PBS for 36 h. (A) Representative Western blotting assay and quantitation of the level of SIRT3 protein. (B) The analysis of SIRT3 deacetylase activity using mitochondrial fractions as described under Materials and Methods. *p < 0.05 versus PBS. #p < 0.05 versus AGEs (100 μg/ml at 36 h). (C) Representative Western blotting assay and quantitation of the level of mitochondrial antioxidants including SOD2, catalase, TRX2 and TRXR2. *p < 0.05 versus PBS. #p < 0.05 versus AGEs (100 μg/ml at 36 h). (D) Representative Western blotting assay and quantitation of the level of SIRT3 protein. *p < 0.05 versus PBS + siCON. #p < 0.05 versus AGEs + siCON. (E) The analysis of SIRT3 deacetylase activity using mitochondrial fractions. *p < 0.05 versus PBS + siCON. #p < 0.05 versus AGEs + siCON. (F) Representative Western blotting assay and quantitation of the level of SIRT3 protein. *p < 0.05 versus PBS + Lenti-Vector (blank vector). #p < 0.05 versus AGEs + Lenti-Vector. (G) The analysis of SIRT3 deacetylase activity using mitochondrial fractions. *p < 0.05 versus PBS + Lenti-Vector. #p < 0.05 versus AGEs + Lenti-Vector. (H) Scrambled siRNA (siCON) or SIRT3 siRNA (siSIRT3) transfection were performed before AGEs treatment (200 μg/ml, 36 h). The SOD2, catalase, TRX2 and TRXR2 protein levels were analyzed and quantitated by Western blotting. *p < 0.05 versus PBS + siCON. #p < 0.05 versus AGEs + siCON. (I) Lenti-Vector or Lenti-SIRT3 infection were performed before AGEs treatment (200 μg/ml, 36 h). The SOD2, catalase, TRX2 and TRXR2 protein levels were analyzed and quantitated by Western blotting. *p < 0.05 versus PBS + Lenti-Vector. #p < 0.05 versus AGEs + Lenti-Vector. (J) Representative fluorescence images with MitoSOX (red) and MitoTracker (green) double-staining. Cell nuclei are stained by DAPI. (K, L) Cell apoptosis was measured by Annexin V-APC/7-AAD staining under flow cytometry analysis. (K) *p < 0.05 versus PBS + siCON. #p < 0.05 versus AGEs + siCON. (L) *p < 0.05 versus PBS + Lenti-Vector. #p < 0.05 versus AGEs + Lenti-Vector.

the NP area by strong SO staining in the PBS-injected groups. Numerous stellar-shaped cells were seen in NP tissue and the annulus fibrosus layer was also well organized. In AGEs-injected groups, the disc height was collapsed, with an evident loss of cells and increased tissue fibrillation in the NP area (Fig. 8B). The boundary of nucleus pulposus and annulus fibrosus was disappeared and the whole layer of annulus fibrosus was disrupted (Fig. 8B). Conversely, additional NMN administration reduced the IVD degenerative changes compared to that in

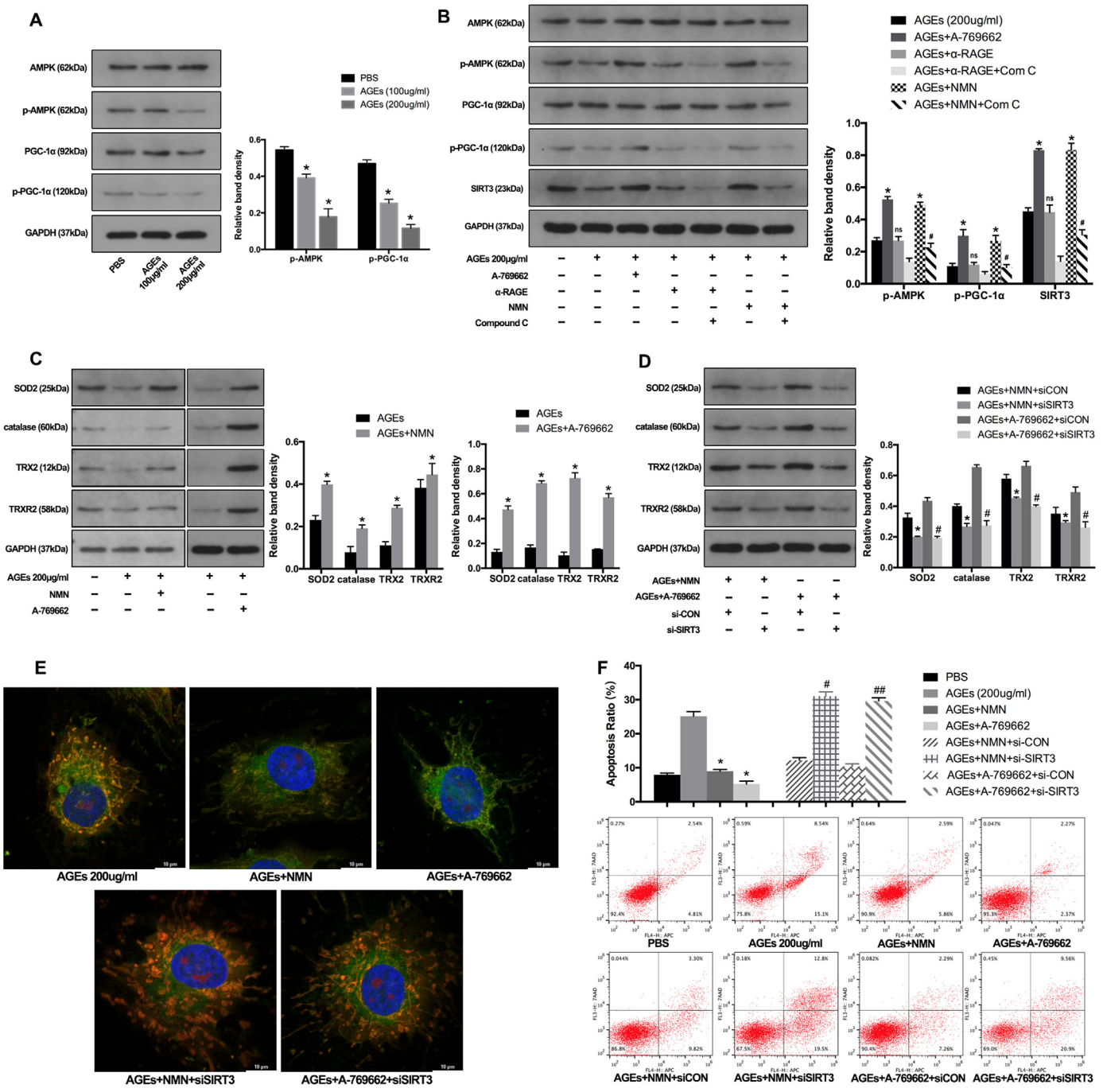

Fig. 7. NMN administration restored SIRT3 function and alleviated oxidative stress and apoptosis in AGEs-treated human NP cells via AMPK/PGC-1α pathway. (A) Human NP cells were treated with AGEs (100–200 μg/ml) or PBS for 36 h. Representative Western blotting assay and quantitation of the levels of AMPK, p-AMPK, PGC-1α, p-PGC-1α proteins. *p < 0.05 versus PBS. (B) Western blotting assay of AMPK, p-AMPK, PGC-1α, p-PGC-1α levels in NP cells stimulated with AGEs (200 μg/ml) in the presence or absence of A-769662 (50 μM), RAGE antibody (10 μg/ml), NMN (100 μM) or Compound C (50 uM). The quantitation of the protein levels: *p < 0.05 versus AGEs (200 μg/ml). *ns* versus AGEs (200 μg/ml). # p < 0.05 versus AGEs + NMN. (C) Western blotting assay of SOD2, catalase, TRX2 and TRXR2 levels in NP cells stimulated with AGEs (200 μg/ml) in the presence or absence of A-769662 (50 μM) or NMN (100 μM). The quantitation of the protein levels: *p < 0.05 versus AGEs. (D) Western blotting assay of SOD2, catalase, TRX2 and TRXR2 levels in siRNA transfected NP cells stimulated with AGEs (200 μg/ml) in the presence or absence of A-769662 (50 μM) or NMN (100 μM). *p < 0.05 versus AGEs + NMN + siCON. #p < 0.05 versus AGEs + A-769662 + siCON. (E) Representative fluorescence images with MitoSOX (red) and MitoTracker (green) double-staining in siRNA transfected NP cells stimulated with AGEs (200 μg/ml) in the presence or absence of A-769662 (50 μM) or NMN (100 μM). (F) Cell apoptosis was measured by Annexin V-APC/7-AAD staining under flow cytometry analysis. *p < 0.05 versus AGEs (200 μg/ml). # p < 0.05 versus AGEs + NMN + siCON. ##p < 0.05 versus AGEs + A-769662 + siCON.

AGEs-injected groups, although some degenerative phenotype still existed. As shown, there was still some loose NP tissue (> 25%) with stellar-shaped cells and glycosaminoglycan content detected by SO staining (Fig. 8C). The boundary of nucleus pulposus and annulus fibrosus was still clear and the disc height was moderate, while the inward half of annulus fibrosus layer was disorganized. Overall, we evaluated the histopathological scores, using a grading scale described previously [44]. The statistical results also confirmed that NMN

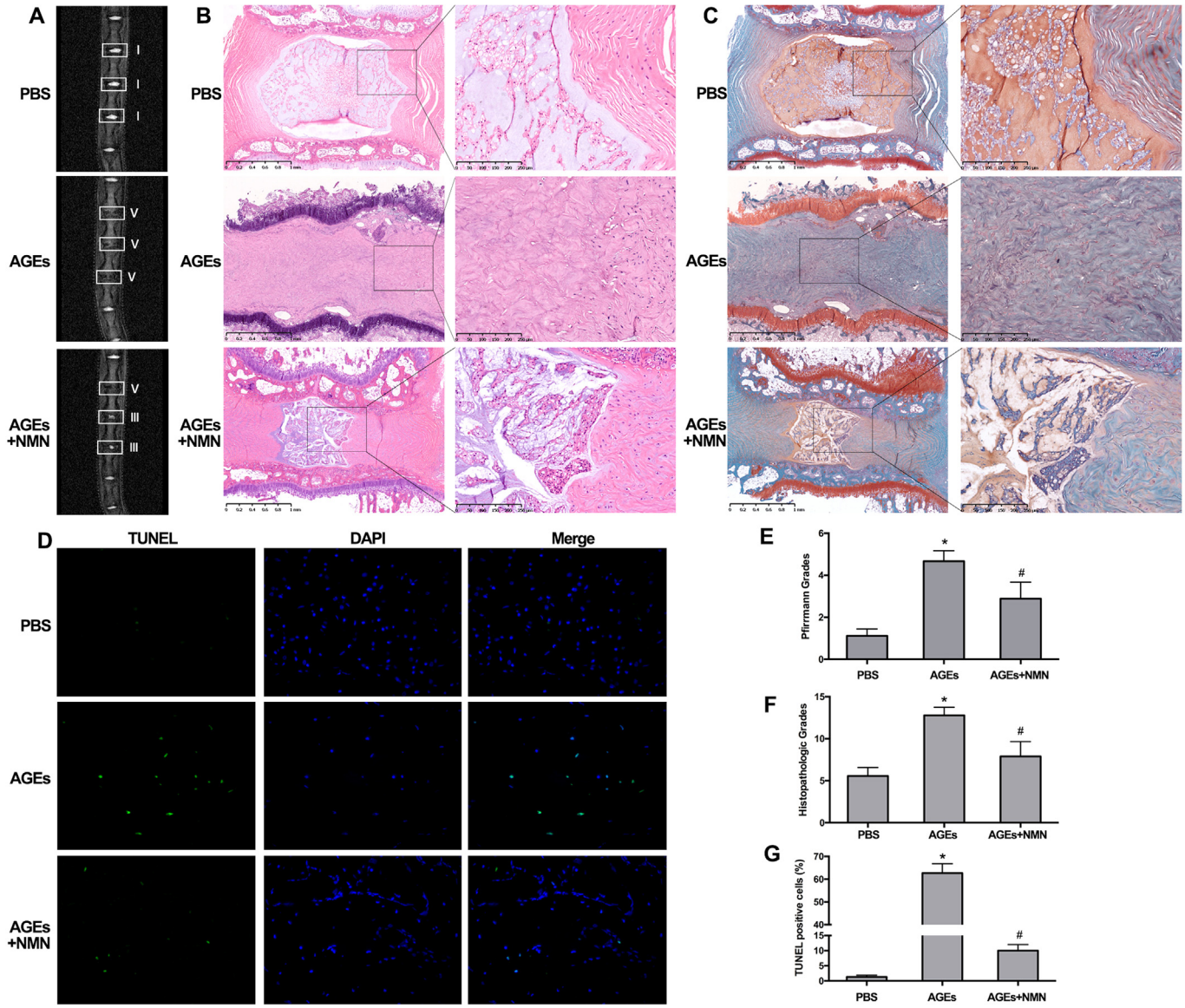

Fig. 8. NMN Administration ameliorated IVD degeneration *in vivo*. The rat tail discs were injected with PBS, AGEs (200 μg/ml), the mixture of AGEs (200 μg/ml) and NMN (100 μM), maintained for one month. (A) Rat tails were examined using MRI at T2-weighted signal and representative MRI images with white squares labeling the operated levels were shown. (B, C) Whole tail discs were observed using HE and SO staining. (D) TUNEL staining and fluorescence microscope analysis were used to detected apoptosis in rat tail discs. The quantitative analysis of degenerative degree using MRI images according to Pfirrmann grade system (E), HE and SO staining images according to histological grading scale (F) and TUNEL fluorescent images by positive cell ratios (G). *$p < 0.05$ versus PBS. #$p < 0.05$ versus AGEs.

administration could ameliorate the AGEs-induced IVD degeneration (Fig. 8F).

Moreover, as described above, AGEs may promote IVD degeneration by inducing NP cell apoptosis. We further performed TUNEL staining in IVD specimens from rats and measured the corresponding ratio of positive staining cells. As shown, AGEs injection increased the positive ratio of TUNEL staining compared to PBS injection, which was attenuated by NMN administration (Fig. 8D and G). The SIRT3 and cleaved-caspase-3 levels were also examined. As expected, both western blotting and immunofluorescence staining revealed that AGEs injection induced SIRT3 levels downregulation and cleaved-caspase-3 upregulation, while NMN administration could alleviate these responses (Fig. S5). Taken together, our in vivo studies further confirmed that NMN administration may restore SIRT3 function and ameliorate AGEs-induced NP cell apoptosis and IVD degeneration.

4. Discussion

Various risk factors have been shown to be involved in apoptosis and the imbalance of anabolic and catabolic activities that drive the development of IVD degeneration [45,46]. Although many efforts have been made to achieve early diagnosis and prevent IVD degeneration and lower back pain disorders [47–49], the therapeutic protocols currently used for treating IVD degeneration-associated diseases are only for relieving symptoms and invalid to recover IVD function, and can cause spinal disability together. In the current study, we identified AGEs as risk molecule associated with IVD degeneration that created an oxidative stress microenvironment and promoted mitochondrial dysfunction and the loss of NP cell viability. Further study showed that the decrease of SIRT3 deacetylation activity played a crucial role in the oxidative stress of NP cells.

Extensive post-translational modification of proteins can affect protein folding and generate micro-anatomical changes in the

proteoglycan–collagen network, which is a hallmark of chronic degenerative and metabolic diseases, including osteoarthritis, osteoporosis, and Alzheimer's disease [50–52]. Several studies have demonstrated that post-translational modification could not only disrupt the mechanical properties of tissues [53], but could also act as damage-associated molecular patterns to induce inflammatory responses and cell death [54,55]. AGEs are the main products of protein post-translational glycosylation. Previous studies have demonstrated that AGEs were significantly deposited in NP cells with increasing age and IVD degeneration, which could enhance inflammatory responses and disrupt the balance between anabolism and catabolism [24,31,56]. In this study, we further demonstrated that AGEs treatment significantly suppressed cell survival and proliferation in NP cells, which played important roles in IVD degeneration. Moreover, data from our in vitro and in vivo studies confirmed that apoptosis was involved in this process.

Mitochondria can intrinsically regulate apoptosis via the involvement of several key events, including the release of proapoptotic molecules such as Cyt-c, Diablo, and HtrA2, which is accompanied by disruption of the electron transport chain and the loss of MMP [57,58]. Although the mechanisms involved in their release are not fully understood, the observations of Bax–Bak oligomerization and translocation to mitochondria suggest the Bcl-2 family of proteins as the best-characterized regulators, which directly modulate mitochondrial outer membrane permeability and Cyt-c release. Other mechanisms, such as mPTP-dependent and serine protease(s)-dependent processes have also received recognition recently [37,59,60]. However, the underlying mechanisms and action manners are complicated and cell type-specific. It is well known that Bax–Bak oligomers mediate the effects of various risk factors that induce NP cell apoptosis [11,14]. Moreover, considering the previous finding that AGEs could induce prolonged mPTP activation [24], we further investigated the release of mitochondrial Cyt-c along with changes in the Bcl-2: Bax ratio and mPTP activation, which indicated that they may induce human NP cell apoptosis through a combined mechanism.

Complex I and III of the mitochondrial respiratory chain are the main production sites of intracellular ROS, which act as important secondary messengers for diverse cellular processes [61]. Increased ROS generation occurred during IVD degeneration and drove NP cell apoptosis and the loss of MMP [11,62]. Further, previous studies also showed that excessive ROS production and oxidative stress are responsible for mPTP- and Bax–Bak-dependent mitochondrial dysfunction and cell death [37,38,63], although this pathway is cell type-specific [64]. MitoTEMPO and SKQ1 were described previously as a mitochondria-targeting antioxidant that could effectively alleviate mitochondrial ROS-originated oxidative stress [37,65]. Thus, the role of ROS in AGEs-induced prolonged mPTP activation and Bax–Bak oligomerization in human NP cells was studied after MitoTEMPO or SKQ1 pre-treatment. As results showed that changes in the ROS level and mitochondrial function were significantly attenuated by MitoTEMPO or SKQ1 pre-treatment, along with mPTP activity, the Bax level, and apoptosis in human NP cells. These results indicated that ROS-mediated intrinsic mitochondrial pathway was involved in AGEs-induced human NP cell apoptosis. Furthermore, RAGE was first identified as the receptor for AGEs and mediated most intracellular signal transduction, including the inflammatory response in human NP cells [24]. Previous studies have reported that RAGE could mediate caspase-8-dependent extrinsic apoptotic pathway in response to AGEs stimulation [33] and the crosstalk between extrinsic and intrinsic pathways may be essential for apoptotic events in some cell types [66]. Therefore, more detailed mechanisms about extrinsic and intrinsic apoptotic pathways and their crosstalk may exist in AGEs-induced human NP cell death and deserve more investigation.

It has been well documented that SIRT3 is involved in various oxidative stress-related diseases, where deficiency or functional impairment was crucial for mitochondrial dysfunction and disease progression [19,20,67]. Considering the important role of oxidative stress and mitochondrial dysfunction in NP cell apoptosis and the unexplored mechanisms, we further investigated SIRT3 function in human NP tissues and its relationships with AGEs-induced oxidative stress and IVD degeneration. A negative correlation was identified between the SIRT3 protein level and the IVD degenerative grade, along with AGEs deposition. Moreover, the disruption of SIRT3 function was also confirmed in AGEs-stimulated human NP cells by performing in vitro experiments. Based on that, we first attempted to genetically manipulate the mitochondrial SIRT3 function to clarify its roles in AGEs-induced human NP cell apoptosis. Initially, an SIRT3-specific siRNA was used to knock down SIRT3 expression in normal and AGEs-induced human NP cells, which resulted in the aggravation of oxidative stress and apoptotic events. Additionally, SIRT3 overexpression by Lenti-SIRT3 could ameliorate mitochondrial ROS levels and cell apoptosis induced by AGEs treatment. These results indicated that the regulation of SIRT3 function by genetic manipulation may have the therapeutic potential for AGEs-associated IVD degeneration, while the gene therapy is accompanied by the inherent potential risks of cancer development and immune responses [68]. Therefore, we further explored the pharmacological interventions. NMN acts as a precursor of NAD^+ that was reported to restore SIRT members [21–23], including SIRT3 [21,42]. In beta cells, the recovery of NAD^+ supplementation with NMN attenuated suppression of the SIRT3 expression by pro-inflammatory cytokines [21]. Similarly, NMN administration also restored the deacetylation activity of SIRT3 in circadian mutant mice [42]. More importantly, NMN administration has undergone clinical trials for some diseases. In this study, we explored its potential application in IVD degeneration and the results showed that NMN administration could protect human NP cell against AGEs-induced oxidative stress and apoptosis, in which restoring SIRT3 function was involved.

The biological relevance of SIRT3 in NP cell apoptosis and IVD degeneration induced by AGEs was also highlighted by in vitro findings showing its role in maintaining the antioxidant network. ROS are the by-products along with the electrons leakage from the electron transfer chain, of which level is typically low under normal physiological conditions and is kept in check by intracellular and intra-mitochondrial scavenging systems. Previous reports have shown that impairment of the mitochondrial antioxidant network occurs in many diseases associated with oxidative stress, which could potentially be reversed by robust SIRT3 function [18,39,69]. In the present study, we observed that restoring SIRT3 function could rescue the mitochondrial antioxidant network suppressed by AEGs treatment, which was also involved in the NMN protective effect.

Furthermore, we demonstrated a close relationship between SIRT3 function and AMPK-PGC-1α pathway in regulating mitochondrial antioxidant network under AGEs stimulation (Fig. 9). Previous studies have reported that AMPK activation could promote the interaction of PGC-1α with estrogen-related receptor alpha that was a crucial transcription factor for SIRT3 expression. Similarly, our present study observed an inhibited “AMPK-PGC-1α” pathway by AGEs treatment. Further utilizing pharmacological manipulation, this study showed for the first time that AMPK-PGC-1α activation by A-769662 could ameliorate the suppressive effect of AGEs on SIRT3 and mitochondrial antioxidant network, while RAGE was not responsible for this process. Moreover, AMPK-PGC-1α pathway was also involved in the protective function of NMN, confirmed by the inhibitory effect of Compound C. These results demonstrated that AMPK-PGC-1α was involved in AGEs-suppressive and NMN-protective effect on SIRT3 and mitochondrial antioxidant network. Previous study reported that AMPK/PGC-1α pathway could limit oxidative stress in osteoarthritis progression. However, whether A-769662 and NMN work in this process by targeting SIRT3 was not clear. Our results using SIRT3 knockdown suggested that SIRT3 was indispensable for the protective effect of AMPK/PGC-1α activation in AGEs-induced human NP cell apoptosis.

In current study, we also established a simple IVD degeneration model in order to further evaluate the effect of AGEs on NP cell survival

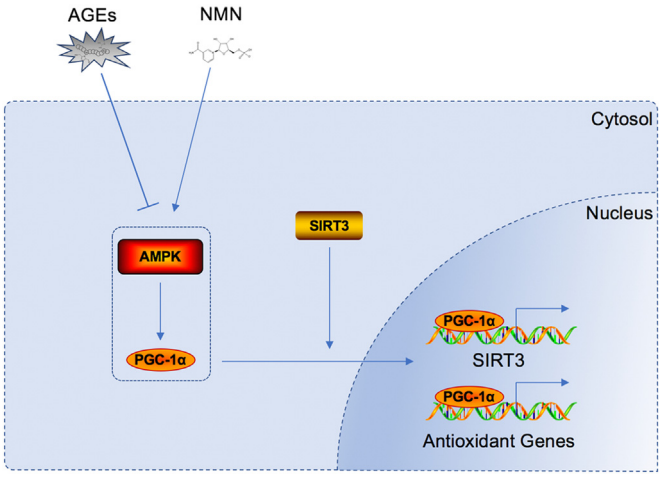

Fig. 9. Schematic model illustrating the signaling pathway by SIRT3 and AMPK-PGC-1α to mediate AGEs-induced and NMN-protective effect on mitochondrial oxidative stress and NP cell apoptosis.

and IVD degeneration and the therapeutic potential of NMN treatment in vivo. The local injection into discs was used to induce AGEs-depositive microenvironment and administer NMN treatment, which was also applied in other disease models [70,71]. As observed, exogenous NMN administration could ameliorate the NP cell apoptosis and IVD degeneration induced by AGEs, along with the restoration of SIRT3 level. Meanwhile, we cannot neglect the limitations that involved in this animal model using local injection into rat tail discs, although it is widely used [14,72]. The rat IVDs experience different biomechanical characteristics with that of human. More studies using monkey, goat or dog may provide further insights. In addition, the AGEs-injection model can simulate its function as bioactive molecules, while it is poor for mimicking the altered mechanical microenvironment by AGEs deposition.

Another limitation of this study was that the use of NMN as pharmacological intervention to regulate SIRT3 function was not specific. Although our present study showed the protective effect of SIRT3 on AGEs-induced NP cell apoptosis and IVD degeneration, more molecules have been targeted by NMN [21–23] and their potential interaction with SIRT3 may be involved in this process and need more mechanistic investigations in the future.

5. Conclusion

The current study represents the first demonstration of the protective role of SIRT3 in IVD degeneration. Previous data showed that aging was one risk factor that promoted SIRT3 down-modulation and osteoarthritis progression [20]. We further clarified that AGEs acted as risk molecule involved in IVD degeneration, and participated in suppressing SIRT3 function and inducing NP cell apoptosis and IVD degeneration, which can result from mitochondrial redox disorder and oxidative stress. Moreover, NMN administration alleviated the AGEs-induced oxidative stress and NP cell apoptosis by restoring SIRT3 function and the mitochondrial antioxidant network. Thus, we infer that SIRT3 function in NP cells can potentially serve as a new and effective therapeutic target for AGEs-associated IVD degeneration.

Acknowledgements

This study was supported by the National Natural Science Foundation of China (81772401, U1603121) and Natural Science Foundation of Hubei Province (WJ2017Z016).

Author's contributions

YS designed the study protocol and wrote the first manuscript; YS, SL and WG conducted the experimental operation; RJL and WL helped to design the study, collected and analyzed data; JT, KW and LK established the animal model; HPY and XHW collected the NP tissue specimen and clinical data. YG, YKZ and CY conducted the surgical operation and extensively reviewed and revised manuscript.

Conflict of interests

All authors have approved the final version of the manuscript and declared that no competing interest exists.

Appendix A. Supplementary material

Supplementary data associated with this article can be found in the online version at doi:10.1016/j.redox.2018.09.006

References

[1] G.B.D. Disease, I. Injury, C. Prevalence, Global, regional, and national incidence, prevalence, and years lived with disability for 328 diseases and injuries for 195 countries, 1990–2016: a systematic analysis for the Global burden of disease study 2016, Lancet 390 (2017) 1211–1259.
[2] M.D. Humzah, R.W. Soames, Human intervertebral disc: structure and function, Anat. Rec. 220 (1988) 337–356.
[3] M.H. Walker, D.G. Anderson, Molecular basis of intervertebral disc degeneration, Spine J. 4 (2004) 158S–166S.
[4] S. Roberts, H. Evans, J. Trivedi, J. Menage, Histology and pathology of the human intervertebral disc, J. Bone Jt. Surg. Am. 88 (Suppl. 2) (2006) S10–S14.
[5] C.Q. Zhao, L.M. Wang, L.S. Jiang, L.Y. Dai, The cell biology of intervertebral disc aging and degeneration, Ageing Res. Rev. 6 (2007) 247–261.
[6] H. Sudo, A. Minami, Regulation of apoptosis in nucleus pulposus cells by optimized exogenous Bcl-2 overexpression, J. Orthop. Res. 28 (2010) 1608–1613.
[7] H. Sudo, A. Minami, Caspase 3 as a therapeutic target for regulation of intervertebral disc degeneration in rabbits, Arthritis Rheum. 63 (2011) 1648–1657.
[8] S.S. Sivan, E. Tsitron, E. Wachtel, P. Roughley, N. Sakkee, F. van der Ham, J. Degroot, A. Maroudas, Age-related accumulation of pentosidine in aggrecan and collagen from normal and degenerate human intervertebral discs, Biochem. J. 399 (2006) 29–35.
[9] B. Scharf, C.C. Clement, S. Yodmuang, A.M. Urbanska, S.O. Suadicani, D. Aphkhazava, M.M. Thi, G. Perino, J.A. Hardin, N. Cobelli, G. Vunjak-Novakovic, L. Santambrogio, Age-related carbonylation of fibrocartilage structural proteins drives tissue degenerative modification, Chem. Biol. 20 (2013) 922–934.
[10] C. Feng, M. Yang, M. Lan, C. Liu, Y. Zhang, B. Huang, H. Liu, Y. Zhou, ROS: crucial intermediators in the pathogenesis of intervertebral disc degeneration, Oxid. Med. Cell. Longev. 2017 (2017) 5601593.
[11] F. Ding, Z.W. Shao, S.H. Yang, Q. Wu, F. Gao, L.M. Xiong, Role of mitochondrial pathway in compression-induced apoptosis of nucleus pulposus cells, Apoptosis 17 (2012) 579–590.
[12] L.A. Nasto, A.R. Robinson, K. Ngo, C.L. Clauson, Q. Dong, C. Croix St, G. Sowa, E. Pola, P.D. Robbins, J. Kang, L.J. Niedernhofer, P. Wipf, N.V. Vo, Mitochondrial-derived reactive oxygen species (ROS) play a causal role in aging-related intervertebral disc degeneration, J. Orthop. Res. 31 (2013) 1150–1157.
[13] X. Cheng, B. Ni, F. Zhang, Y. Hu, J. Zhao, High glucose-induced oxidative stress mediates apoptosis and extracellular matrix metabolic imbalances possibly via p38 MAPK activation in rat nucleus pulposus cells, J. Diabetes Res. 2016 (2016) 3765173.
[14] D. Chen, D. Xia, Z. Pan, D. Xu, Y. Zhou, Y. Wu, N. Cai, Q. Tang, C. Wang, M. Yan, J.J. Zhang, K. Zhou, Q. Wang, Y. Feng, X. Wang, H. Xu, X. Zhang, N. Tian, Metformin protects against apoptosis and senescence in nucleus pulposus cells and ameliorates disc degeneration in vivo, Cell Death Dis. 7 (2016) e2441.
[15] C.X. Zhang, T. Wang, J.F. Ma, Y. Liu, Z.G. Zhou, D.C. Wang, Protective effect of CDDO-ethyl amide against high-glucose-induced oxidative injury via the Nrf2/HO-1 pathway, Spine J. 17 (2017) 1017–1025.
[16] B.J. Morris, Seven sirtuins for seven deadly diseases of aging, Free Radic. Biol. Med. 56 (2013) 133–171.
[17] S. Kumar, D.B. Lombard, Mitochondrial sirtuins and their relationships with metabolic disease and cancer, Antioxid. Redox Signal. 22 (2015) 1060–1077.
[18] N.R. Sundaresan, M. Gupta, G. Kim, S.B. Rajamohan, A. Isbatan, M.P. Gupta, Sirt3 blocks the cardiac hypertrophic response by augmenting Foxo3a-dependent antioxidant defense mechanisms in mice, J. Clin. Investig. 119 (2009) 2758–2771.
[19] M. Morigi, L. Perico, C. Rota, L. Longaretti, S. Conti, D. Rottoli, R. Novelli, G. Remuzzi, A. Benigni, Sirtuin 3-dependent mitochondrial dynamic improvements protect against acute kidney injury, J. Clin. Investig. 125 (2015) 715–726.
[20] Y. Fu, M. Kinter, J. Hudson, K.M. Humphries, R.S. Lane, J.R. White, M. Hakim, Y. Pan, E. Verdin, T.M. Griffin, Aging promotes sirtuin 3-dependent cartilage superoxide dismutase 2 acetylation and osteoarthritis, Arthritis Rheumatol. 68 (2016)

1887–1898.
[21] P.W. Caton, S.J. Richardson, J. Kieswich, M. Bugliani, M.L. Holland, P. Marchetti, N.G. Morgan, M.M. Yaqoob, M.J. Holness, M.C. Sugden, Sirtuin 3 regulates mouse pancreatic beta cell function and is suppressed in pancreatic islets isolated from human type 2 diabetic patients, Diabetologia 56 (2013) 1068–1077.
[22] M.S. Bonkowski, D.A. Sinclair, Slowing ageing by design: the rise of NAD(+) and sirtuin-activating compounds, Nat. Rev. Mol. Cell Biol. 17 (2016) 679–690.
[23] J. Yoshino, K.F. Mills, M.J. Yoon, S. Imai, Nicotinamide mononucleotide, a key NAD(+) intermediate, treats the pathophysiology of diet- and age-induced diabetes in mice, Cell Metab. 14 (2011) 528–536.
[24] Y. Song, Y. Wang, Y. Zhang, W. Geng, W. Liu, Y. Gao, S. Li, K. Wang, X. Wu, L. Kang, C. Yang, Advanced glycation end products regulate anabolic and catabolic activities via NLRP3-inflammasome activation in human nucleus pulposus cells, J. Cell. Mol. Med. 21 (2017) 1373–1387.
[25] A.J. Fields, B. Berg-Johansen, L.N. Metz, S. Miller, B. La, E.C. Liebenberg, D.G. Coughlin, J.L. Graham, K.L. Stanhope, P.J. Havel, J.C. Lotz, Alterations in intervertebral disc composition, matrix homeostasis and biomechanical behavior in the UCD-T2DM rat model of type 2 diabetes, J. Orthop. Res. 33 (2015) 738–746.
[26] S. Illien-Junger, F. Grosjean, D.M. Laudier, H. Vlassara, G.E. Striker, J.C. Iatridis, Combined anti-inflammatory and anti-AGE drug treatments have a protective effect on intervertebral discs in mice with diabetes, PLoS One 8 (2013) e64302.
[27] C.W. Pfirrmann, A. Metzdorf, M. Zanetti, J. Hodler, N. Boos, Magnetic resonance classification of lumbar intervertebral disc degeneration, Spine (Phila. Pa 1976) 26 (2001) 1873–1878.
[28] K. Wang, W. Liu, Y. Song, X. Wu, Y. Zhang, S. Li, Y. Gao, J. Tu, Y. Liu, C. Yang, The role of angiopoietin-2 in nucleus pulposus cells during human intervertebral disc degeneration, Lab Investig. 97 (2017) 971–982.
[29] R. Nakamichi, Y. Ito, M. Inui, N. Onizuka, T. Kayama, K. Kataoka, H. Suzuki, M. Mori, M. Inagawa, S. Ichinose, M.K. Lotz, D. Sakai, K. Masuda, T. Ozaki, H. Asahara, Mohawk promotes the maintenance and regeneration of the outer annulus fibrosus of intervertebral discs, Nat. Commun. 7 (2016) 12503.
[30] X.Y. Cai, Y. Xia, S.H. Yang, X.Z. Liu, Z.W. Shao, Y.L. Liu, W. Yang, L.M. Xiong, Ropivacaine- and bupivacaine-induced death of rabbit annulus fibrosus cells in vitro: involvement of the mitochondrial apoptotic pathway, Osteoarthr. Cartil. 23 (2015) 1763–1775.
[31] T.T. Tsai, N.Y. Ho, Y.T. Lin, P.L. Lai, T.S. Fu, C.C. Niu, L.H. Chen, W.J. Chen, J.H. Pang, Advanced glycation end products in degenerative nucleus pulposus with diabetes, J. Orthop. Res. 32 (2014) 238–244.
[32] Q. Wu, Z.M. Zhong, S.Y. Zhu, C.R. Liao, Y. Pan, J.H. Zeng, S. Zheng, R.T. Ding, Q.S. Lin, Q. Ye, W.B. Ye, W. Li, J.T. Chen, Advanced oxidation protein products induce chondrocyte apoptosis via receptor for advanced glycation end products-mediated, redox-dependent intrinsic apoptosis pathway, Apoptosis 21 (2016) 36–50.
[33] Z. Alikhani, M. Alikhani, C.M. Boyd, K. Nagao, P.C. Trackman, D.T. Graves, Advanced glycation end products enhance expression of pro-apoptotic genes and stimulate fibroblast apoptosis through cytoplasmic and mitochondrial pathways, J. Biol. Chem. 280 (2005) 12087–12095.
[34] J. Kim, O.S. Kim, C.S. Kim, E. Sohn, K. Jo, J.S. Kim, Accumulation of argpyrimidine, a methylglyoxal-derived advanced glycation end product, increases apoptosis of lens epithelial cells both in vitro and in vivo, Exp. Mol. Med. 44 (2012) 167–175.
[35] A. Salic, T.J. Mitchison, A chemical method for fast and sensitive detection of DNA synthesis in vivo, Proc. Natl. Acad. Sci. USA 105 (2008) 2415–2420.
[36] G. Kroemer, L. Galluzzi, C. Brenner, Mitochondrial membrane permeabilization in cell death, Physiol. Rev. 87 (2007) 99–163.
[37] H.L. Liang, F. Sedlic, Z. Bosnjak, V. Nilakantan, SOD1 and MitoTEMPO partially prevent mitochondrial permeability transition pore opening, necrosis, and mitochondrial apoptosis after ATP depletion recovery, Free Radic. Biol. Med. 49 (2010) 1550–1560.
[38] C.C. Wu, S.B. Bratton, Regulation of the intrinsic apoptosis pathway by reactive oxygen species, Antioxid. Redox Signal. 19 (2013) 546–558.
[39] H. Pi, S. Xu, R.J. Reiter, P. Guo, L. Zhang, Y. Li, M. Li, Z. Cao, L. Tian, J. Xie, R. Zhang, M. He, Y. Lu, C. Liu, W. Duan, Z. Yu, Z. Zhou, SIRT3-SOD2-mROS-dependent autophagy in cadmium-induced hepatotoxicity and salvage by melatonin, Autophagy 11 (2015) 1037–1051.
[40] E.D. Schleicher, E. Wagner, A.G. Nerlich, Increased accumulation of the glycoxidation product N(epsilon)-(carboxymethyl)lysine in human tissues in diabetes and aging, J. Clin. Investig. 99 (1997) 457–468.
[41] X. Zhao, F. Petursson, B. Viollet, M. Lotz, R. Terkeltaub, R. Liu-Bryan, Peroxisome proliferator-activated receptor gamma coactivator 1alpha and FoxO3A mediate chondroprotection by AMP-activated protein kinase, Arthritis Rheumatol. 66 (2014) 3073–3082.
[42] C.B. Peek, A.H. Affinati, K.M. Ramsey, H.Y. Kuo, W. Yu, L.A. Sena, O. Ilkayeva, B. Marcheva, Y. Kobayashi, C. Omura, D.C. Levine, D.J. Bacsik, D. Gius, C.B. Newgard, E. Goetzman, N.S. Chandel, J.M. Denu, M. Mrksich, J. Bass, Circadian clock NAD+ cycle drives mitochondrial oxidative metabolism in mice, Science 342 (2013) 1243417.
[43] E. Jazini, A.D. Sharan, L.J. Morse, J.P. Dyke, E.B. Aronowitz, L.K. Chen, S.Y. Tang, Alterations in T2 relaxation magnetic resonance imaging of the ovine intervertebral disc due to nonenzymatic glycation, Spine (Phila. Pa 1976) 37 (2012) E209–E215.
[44] H.J. Mao, Q.X. Chen, B. Han, F.C. Li, J. Feng, Z.L. Shi, M. Lin, J. Wang, The effect of injection volume on disc degeneration in a rat tail model, Spine (Phila. Pa 1976) 36 (2011) E1062–E1069.
[45] M.V. Risbud, I.M. Shapiro, Role of cytokines in intervertebral disc degeneration: pain and disc content, Nat. Rev. Rheumatol. 10 (2014) 44–56.
[46] Z. Li, J. Shen, W.K. Wu, X. Yu, J. Liang, G. Qiu, J. Liu, The role of leptin on the organization and expression of cytoskeleton elements in nucleus pulposus cells, J. Orthop. Res. 31 (2013) 847–857.
[47] A. Lazary, Z. Szoverfi, J. Szita, A. Somhegyi, M. Kumin, P.P. Varga, Primary prevention of disc degeneration-related symptoms, Eur. Spine J. 23 (Suppl 3) (2014) S385–S393.
[48] W. Brinjikji, F.E. Diehn, J.G. Jarvik, C.M. Carr, D.F. Kallmes, M.H. Murad, P.H. Luetmer, MRI findings of disc degeneration are more prevalent in adults with low back pain than in asymptomatic controls: a systematic review and meta-analysis, AJNR Am. J. Neuroradiol. 36 (2015) 2394–2399.
[49] H.J. Wilke, J. Urban, M. Kumin, The benefits of multi-disciplinary research on intervertebral disc degeneration, Eur. Spine J. 23 (Suppl. 3) (2014) S303–S304.
[50] Q. Zhuo, W. Yang, J. Chen, Y. Wang, Metabolic syndrome meets osteoarthritis, Nat. Rev. Rheumatol. 8 (2012) 729–737.
[51] G. Hein, C. Weiss, G. Lehmann, T. Niwa, G. Stein, S. Franke, Advanced glycation end product modification of bone proteins and bone remodelling: hypothesis and preliminary immunohistochemical findings, Ann. Rheum. Dis. 65 (2006) 101–104.
[52] Y. Hong, C. Shen, Q. Yin, M. Sun, Y. Ma, X. Liu, Effects of RAGE-specific inhibitor FPS-ZM1 on amyloid-beta metabolism and AGEs-induced inflammation and oxidative stress in rat hippocampus, Neurochem Res. 41 (2016) 1192–1199.
[53] M. Saito, K. Marumo, Collagen cross-links as a determinant of bone quality: a possible explanation for bone fragility in aging, osteoporosis, and diabetes mellitus, Osteoporos. Int. 21 (2010) 195–214.
[54] C. Ospelt, H. Bang, E. Feist, G. Camici, S. Keller, J. Detert, A. Kramer, S. Gay, K. Ghannam, G.R. Burmester, Carbamylation of vimentin is inducible by smoking and represents an independent autoantigen in rheumatoid arthritis, Ann. Rheum. Dis. 76 (2017) 1176–1183.
[55] N.M. Hanssen, K. Wouters, M.S. Huijberts, M.J. Gijbels, J.C. Sluimer, J.L. Scheijen, S. Heeneman, E.A. Biessen, M.J. Daemen, M. Brownlee, D.P. de Kleijn, C.D. Stehouwer, G. Pasterkamp, C.G. Schalkwijk, Higher levels of advanced glycation endproducts in human carotid atherosclerotic plaques are associated with a rupture-prone phenotype, Eur. Heart J. 35 (2014) 1137–1146.
[56] K. Yokosuka, J.S. Park, K. Jimbo, K. Yamada, K. Sato, M. Tsuru, M. Takeuchi, S. Yamagishi, K. Nagata, Advanced glycation end-products downregulating intervertebral disc cell production of proteoglycans in vitro, J. Neurosurg. Spine 5 (2006) 324–329.
[57] D.R. Green, J.C. Reed, Mitochondria and apoptosis, Science 281 (1998) 1309–1312.
[58] C. Wang, R.J. Youle, The role of mitochondria in apoptosis*, Annu. Rev. Genet. 43 (2009) 95–118.
[59] F.B. Mullauer, J.H. Kessler, J.P. Medema, Betulinic acid induces cytochrome c release and apoptosis in a Bax/Bak-independent, permeability transition pore dependent fashion, Apoptosis 14 (2009) 191–202.
[60] T. Mizuta, S. Shimizu, Y. Matsuoka, T. Nakagawa, Y. Tsujimoto, A Bax/Bak-independentmechanism of cytochrome c release, J. Biol. Chem. 282 (2007) 16623–16630.
[61] W. Wang, H. Fang, L. Groom, A. Cheng, W. Zhang, J. Liu, X. Wang, K. Li, P. Han, M. Zheng, J. Yin, W. Wang, M.P. Mattson, J.P. Kao, E.G. Lakatta, S.S. Sheu, K. Ouyang, J. Chen, R.T. Dirksen, H. Cheng, Superoxide flashes in single mitochondria, Cell 134 (2008) 279–290.
[62] K. Li, Y. Li, J. Mi, L. Mao, X. Han, J. Zhao, Resveratrol protects against sodium nitroprusside induced nucleus pulposus cell apoptosis by scavenging ROS, Int. J. Mol. Med. 41 (2018) 2485–2492.
[63] A.P. Halestrap, A.P. Richardson, The mitochondrial permeability transition: a current perspective on its identity and role in ischaemia/reperfusion injury, J. Mol. Cell. Cardiol. 78 (2015) 129–141.
[64] A.G. Kruglov, K.B. Subbotina, N.E. Saris, Redox-cycling compounds can cause the permeabilization of mitochondrial membranes by mechanisms other than ROS production, Free Radic. Biol. Med. 44 (2008) 646–656.
[65] E. Song, S.V. Ramos, X. Huang, Y. Liu, A. Botta, H.K. Sung, P.C. Turnbull, M.B. Wheeler, T. Berger, D.J. Wilson, C.G.R. Perry, T.W. Mak, G. Sweeney, Holo-lipocalin-2-derived siderophores increase mitochondrial ROS and impair oxidative phosphorylation in rat cardiomyocytes, Proc. Natl. Acad. Sci. USA 115 (2018) 1576–1581.
[66] K. Huang, J. Zhang, K.L. O'Neill, C.B. Gurumurthy, R.M. Quadros, Y. Tu, X. Luo, Cleavage by caspase 8 and mitochondrial membrane association activate the BH3-only protein bid during TRAIL-induced apoptosis, J. Biol. Chem. 291 (2016) 11843–11851.
[67] Y. Zhou, A.C.K. Chung, R. Fan, H.M. Lee, G. Xu, B. Tomlinson, J.C.N. Chan, A.P.S. Kong, Sirt3 deficiency increased the vulnerability of pancreatic beta cells to oxidative stress-induced dysfunction, Antioxid. Redox Signal. 27 (2017) 962–976.
[68] S.B. Blanquer, D.W. Grijpma, A.A. Poot, Delivery systems for the treatment of degenerated intervertebral discs, Adv. Drug Deliv. Rev. 84 (2015) 172–187.
[69] J. Gao, Z. Feng, X. Wang, M. Zeng, J. Liu, S. Han, J. Xu, L. Chen, K. Cao, J. Long, Z. Li, W. Shen, J. Liu, SIRT3/SOD2 maintains osteoblast differentiation and bone formation by regulating mitochondrial stress, Cell Death Differ. 25 (2018) 229–240.
[70] J. Kim, K.M. Kim, C.S. Kim, E. Sohn, Y.M. Lee, K. Jo, J.S. Kim, Puerarin inhibits the retinal pericyte apoptosis induced by advanced glycation end products in vitro and in vivo by inhibiting NADPH oxidase-related oxidative stress, Free Radic. Biol. Med. 53 (2012) 357–365.
[71] S. Umadevi, V. Gopi, V. Elangovan, Regulatory mechanism of gallic acid against advanced glycation end products induced cardiac remodeling in experimental rats, Chem. Biol. Interact. 208 (2014) 28–36.
[72] G. Feng, Z. Zhang, M. Dang, X. Zhang, Y. Doleyres, Y. Song, D. Chen, P.X. Ma, Injectable nanofibrous spongy microspheres for NR4A1 plasmid DNA transfection to reverse fibrotic degeneration and support disc regeneration, Biomaterials 131 (2017) 86–97.